UNIVERSITY OF TARTU

FACULTY OF SCIENCE AND TECHNOLOGY

INSTITUTE OF MOLECULAR AND CELL BIOLOGY

DEPARTMENT OF DEVELOPMENTAL BIOLOGY

Investigating the role of *scribble* alleles in Ras-induced tumorigenesis in *Drosophila melanogaster* eye-antennal imaginal discs

Bachelor's Thesis

12 EAP

Laura Elisabeth Christel Lään

Supervisors:

Professor Osamu Shimmi, PhD

Associate Professor Tambet Tõnissoo, PhD

Tartu 2025

INFO PAGE

Investigating the role of *scribble* alleles in Ras-induced tumorigenesis in *Drosophila melanogaster* eye-antennal imaginal discs

Epithelial tumours are characterized by uncontrolled cell proliferation, often driven by the activation of proto-oncogenes and the inactivation of tumour suppressor genes. While clinical data on tumour progression continues to accumulate, the precise molecular mechanisms linking genetic alterations to pathological outcomes remain incompletely understood. *Drosophila melanogaster* serves as an excellent model organism for studying both developmental biology and disease processes, including tumorigenesis, due to its conserved signalling pathways that regulate cell growth and invasion. This study investigates the interaction between different alleles of the *scribble* gene, a key regulator of apicobasal polarity in epithelial cells, and the oncogene Ras^{V12}, using genetic mosaic analysis in the eye-antennal imaginal discs of *Drosophila*. The primary aim is to assess whether the hypomorphic allele $scrib^{5}$ can preserve tissue organization and control cell proliferation when co-expressed with Ras^{V12}. The results demonstrate that $Scrib^{5}$ and Ras^{V12} act synergistically, leading to pronounced tissue overgrowth and disruption of epithelial architecture.

Key words: Apico-basal polarity, *Drosophila melanogaster*, eye-antennal imaginal discs, Scribble, epithelial morphogenesis

CERCS: B350 Development biology, growth (animal), ontogeny, embryology

***scribble* alleelide rolli uurimine Ras-indutseeritud kasvaja tekkes *Drosophila melanogaster*'i silma-tundla imaginaaldiskides**

Epiteliaalseid kasvajaid iseloomustab rakkude kontrollimatu proliferatsioon, mis on tihti põhjustatud proto-onkogeenide aktivatsioonist ja tuumor suppressorgeenide inaktivatsioonist. Kuigi kliiniliste andmete hulk kasvajate kujunemise kohta järjest suureneb on endiselt geneetiliste muutuste ja patoloogiliste seisundite täpsed molekulaarsed mehhanismid ebaselged. Äädikakärbes (*Drosophila melanogaster*) on hea loommudel uurimaks mitmesuguste haiguste tekkemehhanisme, sealhulgas kasvajate arengut. Mitmed signaalirajad, mis reguleerivad rakkude kasvu ja invasiooni on loomariigis konserveerunud. Antud bakalaureusetöö uurib epiteliaalsete rakkude apiko-basaalse polaarsuse regulaatori *scribble* erinevate alleelide ja onkogeeni Ras^{V12}-ne vahelisi interaktsioone, kasutades geneetilist mosaiikanalüüsi äädikakärbse silma-tundla imaginaaldiskides. Töö eesmärk on hinnata, kas hüpomorfse $scrib^{5}$ alleeli ko-ekspressioon Ras^{V12}-ga säilitab epiteliaalsetele kudedele omase ülesehituse ja rakkude jagunemise regulatsiooni. Töö tulemused näitavad, et $Scrib^{5}$ ja Ras^{V12} toimivad sünergiliselt, viies epiteliaalsete kudede vohamiseni ja muutusteni epiteeli ülesehitus. Tulemustest järeldub, et uuritud valkude kombineeritud ekspression kutsub esile märksa tõsisemad kasvaja-laadsed muutused võrrelduna olukorraga kui on ekspresseeritud ainult Ras^{V12}.

Võtmesõnad: Apiko-basaalne polaarsus, *Drosophila melanogaster*, Scribble, silma-tundla imaginaaldisk, epiteeli morfogenees

CERCS: B350 Arengubioloogia, loomade kasv, ontogenees, embrüogenees

TABLE OF CONTENTS

TERMS AND ABBREVIATIONS

ABP – apico-basal polarity

AJs – adherens junctions

ant – antennae

aPKC – atypical protein kinase C

cDNA – complementary DNA

Crb – Crumbs

CyO – curly

DAPI – 4’,6-diamidino-2-phenylindole

Dlg – Disc-large

DP – disc proper

D/V – dorso-ventral

ECM – extracellular matrix

ey – eyeless

eyg – eyegone

F-actin – actin filaments

FA – formaldehyde

FLP – flippase

FLPase – FLP site specific recombinase

FM – First Multiple

FRT – FLPase recombination target

Gal4 – galactose-responsive yeast transcriptional activator in UAS/Gal4 system

Gal80 – galactose-responsive temperature-sensitive repressor of Gal4

GFP – green fluorescent protein

GPCRs – G-protein coupled receptors

GUK – guanylate kinase

HDR – homology-directed repair

he – head epidermis

LAP – LRR (leucine-rich repeat) and PDZ (Postsynaptic density-95, Disc-large, and ZO-1)

Lgl – Lethal giant larvae

LRRs – leucine-rich repeats

M – margin

MAGUK – membrane-associated guanylate kinase

MAPK – mitogen-activated protein kinase

MARCM – mosaic analyses with a repressible cell marker

MF – morphogenetic furrow

mp – maxillary palps

NGS – Normal Goat Serum

nTSGs – neoplastic tumor suppressor genes

oc – ocelli

Par – partitioning defective

Patj – protein associated with tight junction

Pax – Paired box

PDZ – Postsynaptic density-95, Disc-large, and ZO-1

PE – peripodial epitelium

RNAi – RNA interference

RT – room temperature

RTKs – receptor tyrosine kinases

Scrib – Scribble

Sdt – Stardust

SH3 – Src homology 3

SJs – septate junctions

SM – Second Multiple

Tb – Tubby

TCGA – The Cancer Genome Atlas

TM – Third Multiple

toe – twin of eyegone

toy – twin of eyless

TSGs – tumor suppressor genes

UAS – upstream activating sequence

WD40s – tryptophan–aspartic acid 40 residue repeats

WT – wild-type

ZA – zonula adherens

INTRODUCTION

Drosophila melanogaster is a widely used model organism in biological research, due to its short generation time, compact genome, and cost-effective maintenance. It has proven especially valuable in studying developmental biology, genetics, and disease mechanisms, including tumours (Hales et al., 2015; Roote & Prokop, 2017). *Drosophila melanogaster* shares many conserved signalling pathways with mammals, making it a powerful system for investigating the molecular basis of tumourigenesis. Key oncogenes and tumour suppressor genes, such as Ras and Scribble-complex, are functionally conserved between flies and humans (Mirzoyan et al., 2019; Wodarz & Näthke, 2007).

Epithelial tumours are marked by uncontrolled cell proliferation, often resulting from the activation of proto-oncogenes and the inactivation of tumour suppressor genes (Mirzoyan et al., 2019). In epithelial tissues, apicobasal polarity is a key element for maintaining structure and function (Knust, 2000). Disruption of this polarity is a common feature of tumour cells and is associated with the loss of cell-cell adhesion and tissue organization (Mirzoyan et al., 2019). The Scribble protein, a core component of the apicobasal polarity machinery, has been implicated in both polarity regulation and tumour suppression (Bilder et al., 2000; Flores-Benitez & Knust, 2016).

This study explores the interaction between a hypomorphic allele of *scribble* (*scrib*^{5}) and the activated proto-oncogene *Ras* (*Ras*^{V12}) in the eye-antennal imaginal discs of *Drosophila melanogaster*. Using genetic mosaic analysis, the research aims to determine whether Scrib^{5} can maintain epithelial organization and regulate cell proliferation when co-expressed with Ras^{V12}. The theoretical component of the thesis provides an overview of *Drosophila melanogaster* as a model organism, the development of eye-antennal imaginal discs, and the genetic tools used in tumour biology research. The results show that Scrib^{5} and Ras^{V12} act synergistically, leading to significant tissue overgrowth and disruption of epithelial architecture. These findings suggest that the mutated Scribble protein is insufficient to maintain apico-basal polarity and tissue homeostasis in the presence of oncogenic Ras, resulting in a more severe tumour-like phenotype than Ras^{V12} alone. This thesis was conducted in the developmental biology lab at the Institute of Molecular and Cell Biology at the University of Tartu.

1. LITERATURE REVIEW

1.1 *Drosophila melanogaster* as a model organism

Drosophila melanogaster (hereafter referred to as *Drosophila* or fruit fly), commonly known as the fruit fly, is a small insect belonging to the order *Diptera* and the family *Drosophilidae.* It lives on most continents of Earth except Antarctica (Hales et al., 2015). *Drosophila* has served as a model organism for various research, including studies about different diseases and their mechanisms, as well as cellular and molecular mechanisms, particularly in fields such as genetics, developmental biology, and neurobiology. Many aspects make *Drosophila* a good model organism. One key advantage is its genetic similarity to mammals, including humans (Roote & Prokop, 2017). The fruit fly's genome is compact, easily manipulated, and contains many homologs of genes associated with human diseases (Hales et al., 2015). Approximately 60% of the *Drosophila* genome is homologous to the human genome, and about 75% of disease-related genes in humans have counterparts in *Drosophila* (Mirzoyan et al., 2019). Fruit flies are also easy and relatively inexpensive model organisms to maintain and use in experiments, and their short generation time allows research to progress rapidly (Roote & Prokop, 2017).

1.1.1 The life cycle of *Drosophila melanogaster*

Drosophila has a short life cycle that consists of four stages: embryonic stage, larval stage, pupal stage, and adult stage (Figure 1). At 25 °C, this process takes about 9–10 days, but this duration can be adjusted by changing the temperature. For example, at 18 °C, this period is longer, taking about 19 days to develop from a fertilized egg to an adult fly (Hales et al., 2015; Roote & Prokop, 2017). After mating, female flies store spermatozoa in their *receptaculum seminis*, and the sperm can fertilize an egg in the common oviduct. While many sperm may enter the egg, only one takes part in fertilization. After a sperm enters the egg, the meiotic division of the egg is finalized, and the sperm nucleus fuses with the egg nucleus to form a zygote nucleus, which goes through a division and is the starting point of embryonic development (Demerec & Kaufman, 1996). The female fly lays the fertilized eggs shortly after fertilization, after which the zygote requires about 24 hours to complete embryogenesis and develop into a hatched larva (Demerec & Kaufman, 1996; Hales et al., 2015). The post-embryonic larval stage consists of 3 different instar stages (the first, second, and third instar, respectively) before they enter the pupal stage (Hales et al., 2015; Figure 1). At the end of the first and second instar, the larva undergoes molting, shedding the entire cuticle of the insect, including specialized cuticular structures, and the mouth armature (Demerec & Kaufman, 1996;

Parvathi V et al., 2009). During each molt, many structures are reconstructed, during which the organs, e.g., muscles and intestines, grow by an increase in cell size, rather than in cell numbers, while imaginal discs grow through cell multiplication and the cell size remains about the same (Parvathi V et al., 2009). The larval stage typically lasts 5 days to develop into the next stage, the pupal stage (Hales et al., 2015). During pupariation, the larva undergoes metamorphosis, forming a puparium (a hard, protective chitin-based pupal case) from the outer larval cuticle, the last larval skin, which is white and soft at first, but darkens and hardens as development progresses (Demerec & Kaufman, 1996; Figure 1). The pupal stage lasts 4–5 days, during which the larval tissues break down and adult tissues begin to form. Most adult tissues develop from 19 different imaginal discs (Hales et al., 2015), for example, the eye-antennal imaginal discs give rise to the compound eyes, ocelli, maxillary palps, head epidermis, antennae, and bristles (Weasner & Kumar, 2022), and the wing imaginal discs form the adult wings, and also a part of the notum of the adult fly. Other tissues, e.g., the hypodermis of the abdomen, are formed by segmentally arranged imaginal cells and histoblasts. After the adult flies emerge from the pupal case, it takes them 8 to 12 hours to reach sexual maturity, after which the entire cycle restarts (Hales et al., 2015; Parvathi V et al., 2009).

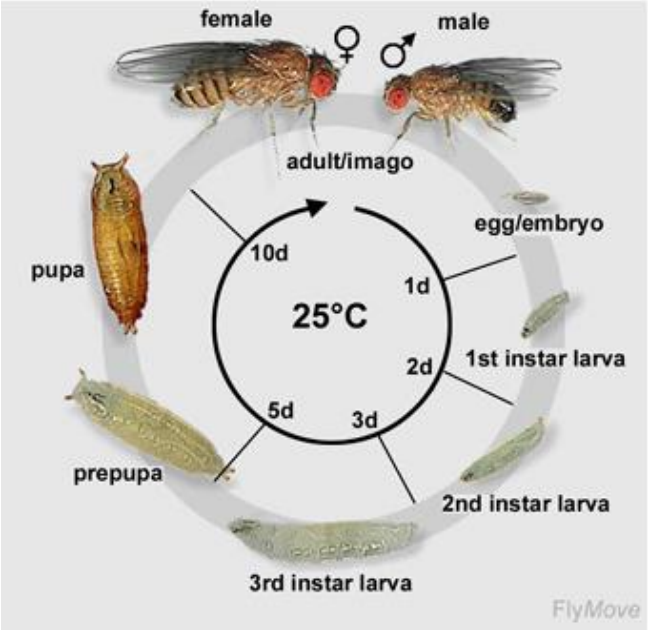

Figure 1. Life cycle of *Drosophila melanogaster.* At 25 °C, the development of a fruit fly from embryo to an adult takes about 9–10 days (d). The life cycle of *Drosophila* begins when a female fly lays eggs, which are then fertilized by sperm cells. It takes approximately 24 hours after fertilization for the resulting embryo to develop into a larva. The larval stage consists of three distinct phases called the first, second, and third instars. The first and second instars each last about 24 hours, while the third instar takes approximately 2 days to develop into a pupa. The pupal stage lasts about 4–5 days, during which the larval tissues undergo metamorphosis to develop the tissues of an adult fly. After the pupal stage, the adult fly emerges from the pupal case. It then takes approximately 8–12 hours for the adult flies to reach sexual maturity, allowing the lifecycle to begin again. Adapted from Roote & Prokop, (2017).

1.1.2 Genome of *Drosophila*

The genome of *Drosophila melanogaster* consists of 4 chromosome pairs and is approximately 180 Mb long (Bosco et al., 2007; Hales et al., 2015; Figure 2). One pair comprises the sex chromosomes: the acrocentric X and the submetacentric Y, both of which are mainly composed of heterochromatin. The other chromosome pairs are autosomes, the second and third being large metacentric, and the fourth a very small autosome (Hales et al., 2015). The second and third chromosomes are divided by centrosomes into right (R) and left (L) arms, referred to as 2L, 2R, 3L, and 3R. The genome of *Drosophila* was first assembled in the year 2000, and ~13,600 genes were identified (Hales et al., 2015; Roote & Prokop, 2017). Most of these genes are named after their mutant phenotypes rather than their wild-type functions (Hales et al., 2015).

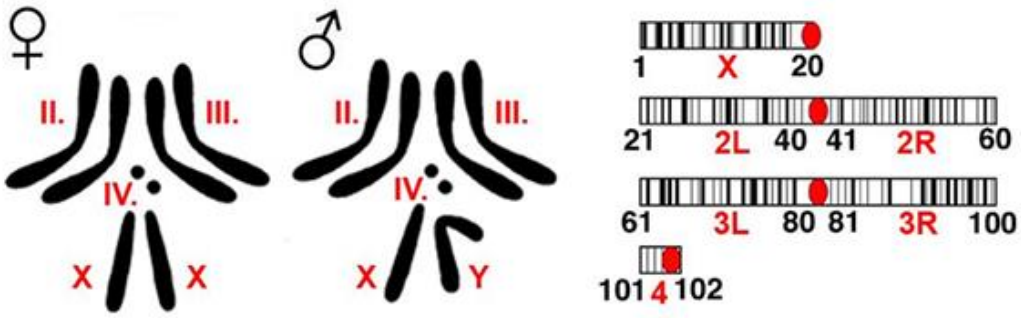

Figure 2. Schematic representation of *Drosophila melanogaster* chromosomes. On the left: The genome of *Drosophila* consists of 4 chromosome pairs. One of which is the sex chromosome pair, including the acrocentric X chromosome, and the submetacentric Y chromosome, which is gene-poor and mainly composed of heterochromatin. The other three chromosome pairs are autosomes. The second (II) and third (III) chromosome pairs are large metacentric, while the fourth (IV) chromosome, also referred to as the dot chromosome, is a small autosome. On the right: a schematic illustrates the *Drosophila* salivary gland polytene chromosomes, displaying a reproducible banding pattern, which can be used for the cytogenetic mapping of gene loci (the black numbers). The second and third chromosomes are subdivided by the centrosome (red dot) into right and left arms (2R, 2L, 3R, and 3L). Adapted from Roote & Prokop, (2017).

1.1.3 Balancer chromosomes

Often in designing mating schemes for experiments with *Drosophila* and maintaining mutant fly stocks, balancer chromosomes are used. Balancer chromosomes, also known as balancers, are described by Roote and Prokop (2017) as "chromosomes which carry multiple overlapping inversions through which the relative positions of genes have been significantly rearranged". Balancer chromosomes are made with multiple inversions and rearrangements, which work to suppress recombination and slow the recovery of recombinant products. Balancer chromosomes undergo segregation during meiosis, but they suppress recombination with a normal sequence chromosome (Miller et al., 2019). Even if recombination does occur, its products are lethal due to duplications and deletions of chromosome fragments. These mechanisms allow for easy maintenance of mutations, transgenes, chromosomal aberrations, etc., in the stock. In order to keep the homologous chromosomes in stock populations while maintaining mutations on the homologs, the presence of recessive lethal or sterile mutations is assured by the balancers (Miller et al., 2019; Roote & Prokop, 2017).

In *Drosophila*, all the chromosomes, apart from the fourth, dot chromosome, and the Y chromosome, have balancer chromosomes available. X chromosome balancers are, for example, First Multiple one (FM1), and FM7c. Second chromosome balancers are Second

Multiple (SM) 1, SM5, SM6a, and Curly (CyO). And third chromosome balancers are, for example, Third Multiple (TM) 3, TM6, and TM6B (Miller et al., 2016, 2018).

1.2 Eye-antennal imaginal discs

The primary imaginal discs in the larvae responsible for developing the head of an adult fly are the eye-antennal imaginal discs. They give rise to several key structures, including the compound eyes and ocelli, which make up the visual system, the antennae and maxillary palps, which form the olfactory system, the head epidermis, and bristles. Since the compound eyes are important for viability and their structural changes are easy to detect, the eye-antennal imaginal discs, as well as the adult fly's compound eyes, have emerged as fundamental models in studies of genetics and developmental biology (Weasner & Kumar, 2022).

1.2.1 Structure of the eye-antennal imaginal disc

The eye-antennal imaginal disc consists of two distinct cell layers, but three different types of epithelial cells, based on their morphology and function (Figure 3). One of the cell layers is called the disc proper (DP), a pseudostratified epithelium that consists of columnar cells. This is covered by the second epithelial cell layer, called the peripodial epithelium (PE), consisting of squamous cells (Weasner & Kumar, 2022). While DP cells are narrow and tall, PE cells have a flattened and broader morphology (Atkins & Mardon, 2009). The DP and PE are joined together by a strip of cuboidal cells, which is called the margin (M), forming a sack-like or a closed pillowcase-like structure (Figure 3c). The eye-antennal disc is divided into six distinct regions, from which the compound eye (eye), the ocelli (oc), the antennae (ant), the maxillary palps (mp), and the surrounding head epidermis (he) develop (Weasner & Kumar, 2022; Figure 4).

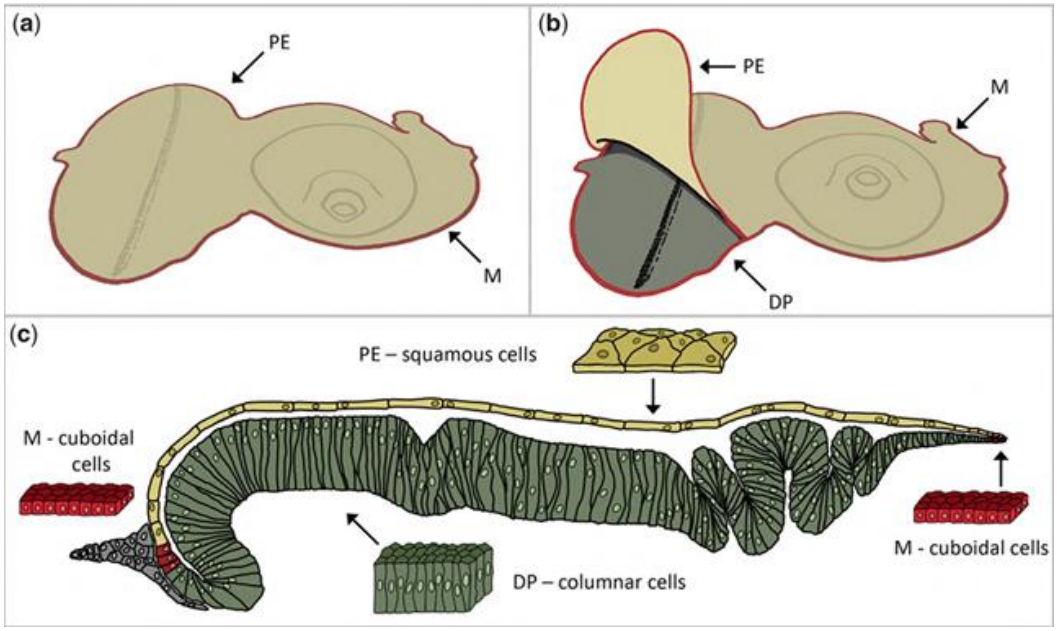

Figure 3. The structure of the eye-antennal imaginal disc. (a, b) Top view of eye-antennal disc. The disc consists of three distinct cell layers: the disc proper (DP), the peripodial epithelium (PE), and the margin (M). (c) The cross-section of the eye-antennal disc. The DP and PE are epithelial cell layers, the DP is a pseudostratified epithelium that consists of columnar cells, while the PE consists of squamous cells. The two epithelial cell sheets are joined by the margin, which is a strip of cuboidal cells, forming a pillowcase-like structure. Adapted from Weasner & Kumar, (2022).

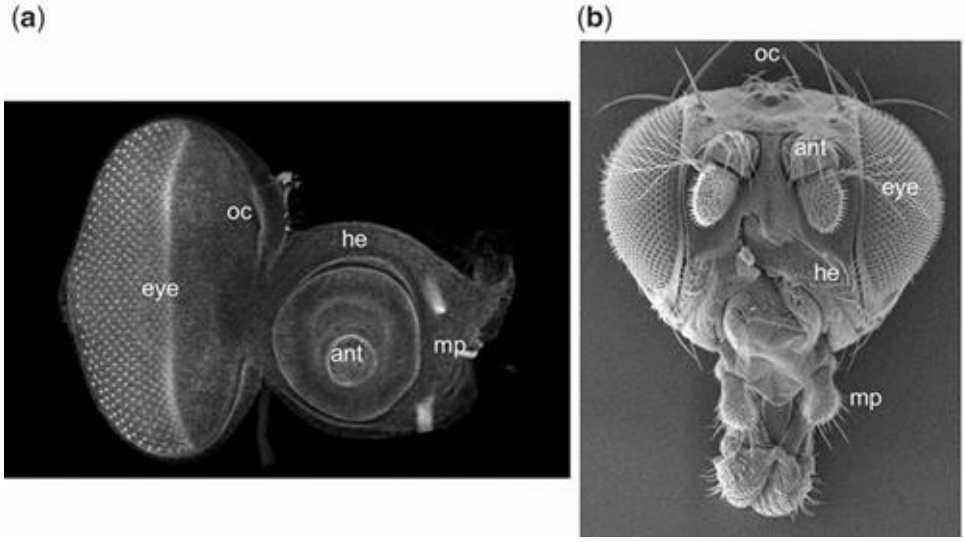

Figure 4. **Fate map of the eye-antennal disc and adult head of *Drosophila*.** (a) Front view of the right eye-antennal imaginal disc, where 6 different regions are clearly observed. (b) Front view of the adult head of *Drosophila*. From specific regions of eye-antennal discs, the adult fly's eyes (eye), ocelli (oc), antennae (ant), maxillary palps (mp), and the surrounding head epidermis (he) are developed. Adapted from Weasner & Kumar, (2022).

1.2.2 Development of eye-antennal imaginal discs

The eye-antennal discs start developing already during the embryonic stage. Its precursors can be identified in stage 13 embryos, and the eye-antennal imaginal disc as a single unit in stage 16/17 embryos (Younossi-Hartenstein et al., 1993). Paired box (Pax) transcription factors play a crucial role in the eye-antennal disc development process. These include *eyeless (ey), twin of eyeless (toy), eyegone (eyg),* and *twin of eyegone (toe)*. Deletion of these genes either individually or in combinations leads to the complete loss of the compound eyes or the entire head of adult flies (Weasner & Kumar, 2022). In the embryonic stage, about 20 cells of the eye-antennal disc are assigned to become the eye cells. Through cell division, the number of cells increases throughout the larval stages, and at the end of the third instar larval stage, this number of cells reaches around 10,000. Then the differentiation of the cells begins to form photoreceptor cells and the ommatidia. During the pupal stage, the cells finalize the differentiation and take their final shapes, forming the eyes of an adult fly (Hales et al., 2015).

1.3 Epithelial tissue structure

The epithelium is a type of tissue that covers both the internal and external surfaces of the body. It lines body cavities and hollow organs and is a crucial tissue in glands. It protects the organism from various harmful factors, such as pathogens, and helps absorb nutrients while excreting waste. Due to different environmental challenges that epithelial tissues face, about 90% of cancers in humans are of epithelial origin (Wang et al., 2012).

Epithelial tissues have complex and diverse cellular architecture. To understand the formation and function of epithelial cells, tissue morphogenesis needs to be understood and studied (Wang et al., 2012).

1.3.1 Epithelial morphology and morphogenesis

Most tissues in an organism develop through epithelial morphogenesis, which consists of three distinct steps. During this process, three-dimensional structures are formed from a simple, flat epithelial sheet. The first step of morphogenesis involves establishing spatial information across the tissue through morphogen gradients or other signals. Then the cells recognize this spatial information, allowing them to differentiate into certain cell types with distinct gene-expression profiles. Finally, the tissues finalize their shape and structure through the cells' specific genetic expression and the cells' interaction with their neighbours (Osterfield et al., 2017).

Drosophila melanogaster develops from an embryo into a larva, and from a larva into an adult fly through metamorphosis during the pupa stage. Throughout this process, the imaginal disc tissues undergo morphogenesis to form an adult fly's eyes, wings, head, etc. (Atkins & Mardon, 2009; Figure 5). In the first instar larva, the eye-antennal imaginal discs are composed of about 20–25 cells, and throughout the larval stages, the number of cells increases as the disc grows and undergoes morphogenesis (Figure 5). The morphogenetic furrow (MF) develops from the beginning to the end of the third instar larval stage and moves while the disc's cells undergo differentiation, leading to the development of the cells fated to form the fly's eyes (Atkins & Mardon, 2009; Figure 5).

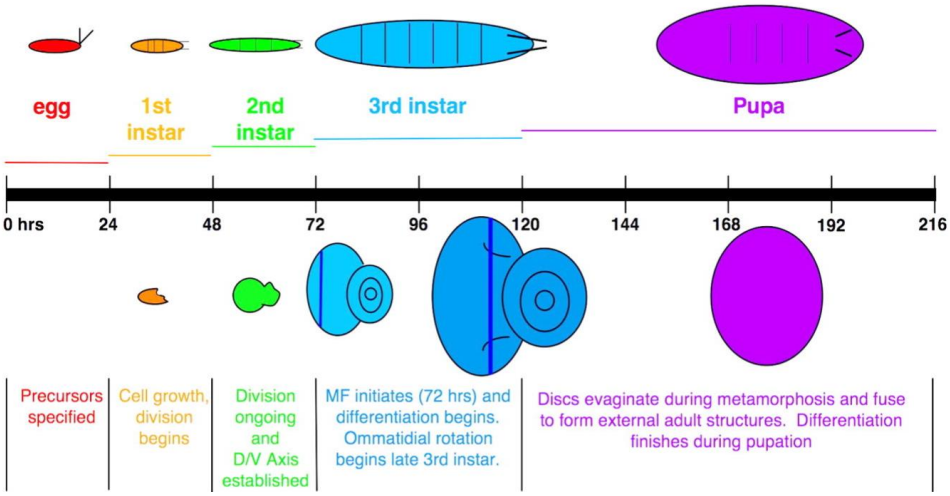

Figure 5. Morphogenesis of the eye-antennal imaginal disc. In the schematic, *Drosophila*'s development from fertilized egg to pupa, showing the relative growth over time, is shown above the timeline. The growth of the eye-antennal imaginal disc is shown under the timeline. The central black line shows the passage of time in hours. Key details of the growth events are written out at the bottom of the schematic. During embryonic development (red), the precursors of the eye-antennal imaginal disc are specified; this process takes about 24 hours. Then the eye-antennal imaginal disc as a distinct structure starts to further develop from the beginning of the first instar larva stage (orange), when the disc is composed of about 20–25 cells. Throughout the larval stage, the eye-antennal disc's cells undergo cell division and growth, this process begins at the first instar stage. During the second instar stage (green), the eye disc cells start to proliferate, the dorso-ventral (D/V) axis is specified, and the antennal disc becomes distinct. At the beginning of the third instar stage (blue), the morphogenic furrow (MF) initiates at the posterior margin (indigo line). The disc continues to grow, while the differentiation of the cells occurs progressively throughout the third instar larva stage. By the late third instar, the MF has crossed most of the eye field, and most of the future eye cells have finished differentiation. During the pupal stage (violet), the imaginal discs break down and start forming the tissues of the adult fly's eye, through metamorphosis. The final steps of differentiation are completed during pupariation. Adapted from Atkins & Mardon, (2009).

As most structures from the eye-antennal imaginal disc develop from the DP, the PE contributes cells to the DP during the development of the disc. Although the PE does contribute to the formation of some structures, including maxillary palps, the vibrissae, etc., and the margin cells derived from the PE play an important role in the initiation of the MF by signalling cell growth and establishing the polarity of the ommatidia (Atkins & Mardon, 2009).

1.3.2 Epithelial polarity

In eukaryotic cells, polarity is essential for maintaining cell shape, the distribution of organelles and proteins, and the orientation of the cytoskeleton (Knust, 2000). Apico-basal polarity (ABP) is the asymmetry along the apical-basal cell axis, and ABP is crucial for maintaining tissue function and homeostasis during development (Flores-Benitez & Knust, 2016; Huang et al., 2023).

Epithelial cell membranes are divided into four distinct cortical domains: apical, basal, junctional, and lateral (St Johnston & Sanson, 2011; Figure 6c). The apical membrane is on the cell surface and faces the organ lumen or the external environment (Flores-Benitez & Knust, 2016). The basal domain connects to the basement membrane and extracellular matrix (ECM) via integrins (Wang et al., 2012). The lateral and junctional membranes contact with the neighbouring cells (Flores-Benitez & Knust, 2016) binding the cells together with junctional complexes, for example, adherens junctions (Figure 6). Apical junctional complexes are also important for maintaining the asymmetric distribution of membrane proteins (Wang et al., 2012).

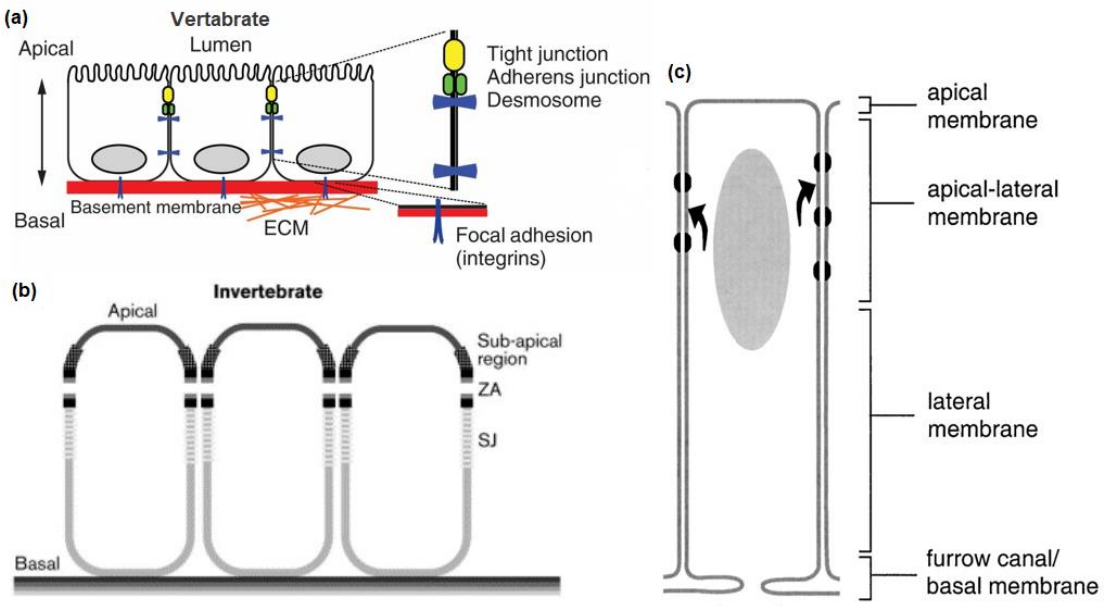

Figure 6. Apico-basal polarity of epithelial cells. Epithelial cell membranes are divided into four distinct cortical domains: apical, basal, apical-lateral (junctional), and lateral membranes. (a) The apical membrane faces the organ lumen, the basal domain is connected to the basement membrane and extracellular matrix (ECM) via integrins. The lateral membrane contacts neighbouring cells, and junctional complexes, e.g., tight junctions and adherens junctions in vertebrates (a, c), and in invertebrates (b), through the zonula adherens (ZA), an actin belt, where E-cadherin is linked to the actin filaments, adherens junctions, and septate junctions (SJ). Image (b) adapted from Knust, (2000); image (c) modified from Tepass et al., (2001); image (a) modified from Wang et al., (2012).

To form cells into tissues, the cells need a coordinated integration of polarizing cues. Firstly, cells must sense their environment and their relation to neighbouring cells. For example, cells can interact directly with the extracellular matrix (ECM) through integrins, allowing them to sense and modify the chemical composition, assembly, etc. of the ECM. Adhesion molecules (e.g., cadherins) and the sensing of diffusible factors (e.g., morphogens, chemoattractants) also play a part in cells interacting with their neighbouring cells. Through these interactions, the cells can initiate their polarity and start assembling into groups. Secondly, the polarity complexes come into play. For the establishment of the tissues' asymmetric organization axis, the cells need to coordinate the asymmetric distribution of polarity complexes. Through these steps, the individual cells can obtain asymmetric polarity (Bryant & Mostov, 2008).

There are three major polarity protein complexes that play a part in cell polarization, and their segregation into apical and basolateral domains is important for cell morphology, tissue physiology, and cell signalling (Bilder & Perrimon, 2000; Flores-Benitez & Knust, 2016). These polarity protein complexes are the Par-complex, the Crb-complex, and the Scrib-complex. The Par-complex consists of proteins partitioning defective (Par) 3/Par6/ atypical

protein kinase C (aPKC). The Crb-complex is composed of proteins Crumbs (Crb), the scaffolding proteins Stardust (Sdt), *Drosophila* Patj (protein associated with tight junction), and *Drosophila* Lin7, and the Scrib-complex is comprised of Scribble (Scrib), Disc-large (Dlg), and Lethal giant larvae (Lgl) (Flores-Benitez & Knust, 2016). Mutations in these proteins cause tissue overproliferation, the loss of cell polarity, tissue architecture, and differentiation (Bilder, 2004; Mirzoyan et al., 2019).

1.3.3 Scribble complex

The Scribble complex is composed of three polarity proteins: Scribble (Scrib), Disc large (Dlg), and Lethal giant larvae (Lgl), and these proteins are located at the baso-lateral membrane domains (Flores-Benitez & Knust, 2016; Mirzoyan et al., 2019). The Scribble complex proteins Scrib, Dlg, and Lgl are also known as neoplastic tumor suppressor genes (nTSGs), and they were first discovered in screens for mutations that cause tumor-like overgrowth in *Drosophila* larval imaginal discs (Wodarz & Näthke, 2007).

In *Drosophila*, tumor suppressor genes (TSGs) are defined as genes whose mutations cause tissue overgrowth (tumors) due to uncontrolled cell proliferation. Tumors caused by mutations of fly TSGs are divided into two groups: hyperplastic and neoplastic. Even though tissues (e.g., imaginal discs) containing hyperplastic tumors are caused by increased proliferation and cell count, they still maintain normal tissue architecture, patterning, and polarity and ultimately develop into adult tissues. Neoplastic tumors, which are caused by mutations in Lgl, Dlg, and Scrib, on the other hand, cause the loss of the ability to organize an epithelial monolayer. In imaginal discs, the loss of Scrib, Dlg, or Lgl results in immense overproliferation and loss of polarity. Neoplastic tumor cells become rounded in shape, pile up on one another, and are unable to complete differentiation (Bilder, 2004; Wodarz & Näthke, 2007).

The nTSG Scrib encodes a LAP (LRR and PDZ) family protein, which is a membrane-associated scaffolding protein with multi-PDZ (Postsynaptic density-95, Disc-large, and ZO-1) domains and leucine-rich repeats (LRRs). Scrib is characterized by 16 LRRs at the N-terminus and four PDZ domains (Bilder, 2004; Bilder & Perrimon, 2000; Figure 7). LRRs are important for protein-protein interactions, they are necessary for Scrib function, and in some instances, can even rescue the functions of Scrib (Bilder, 2004). PDZ domains are also protein-protein interaction domains. They usually bind to the other protein's C-terminus, but each PDZ domain has its own binding preference (Ernst et al., 2014). In Scrib, the PDZ domains play a part in organizing multiprotein complexes in both neurons and epithelial cells as the main integration

sites for molecular networks (Bonello & Peifer, 2019). Scrib is located at the baso-lateral membrane domains, and it is a crucial part of the junctional network, since it is found in association with septate junctions (SJs) and adherens junctions (AJs). Scrib also plays an important part in maintaining epithelial ABP and integrity. (Bilder, 2004; Bilder & Perrimon, 2000; Bonello & Peifer, 2019).

In addition to Scrib, there are two other nTSGs: Dlg and Lgl. Dlg is a MAGUK (membrane-associated guanylate kinase) family protein. It consists of three PDZ domains, a Src homology 3 (SH3) domain, and a guanylate kinase-like (GUK) domain, while Lgl does not have an obvious scaffold, and the only structural homologies it has are tryptophan–aspartic acid 40 residue repeats (WD40s) (Bilder, 2004; Bonello & Peifer, 2019; Figure 7). Similar to Scrib, Dlg is also located at the basolateral domain of an epithelial cell, whereas Lgl does not have a specific location along the apico-basal axis of epithelia, but like Scrib and Dlg, it is found at cell membranes. In a developing epithelia, Dlg is associated with the SJs and AJs, whereas in the mature epithelia, Dlg can be mainly found associated with the SJs (Bilder, 2004).

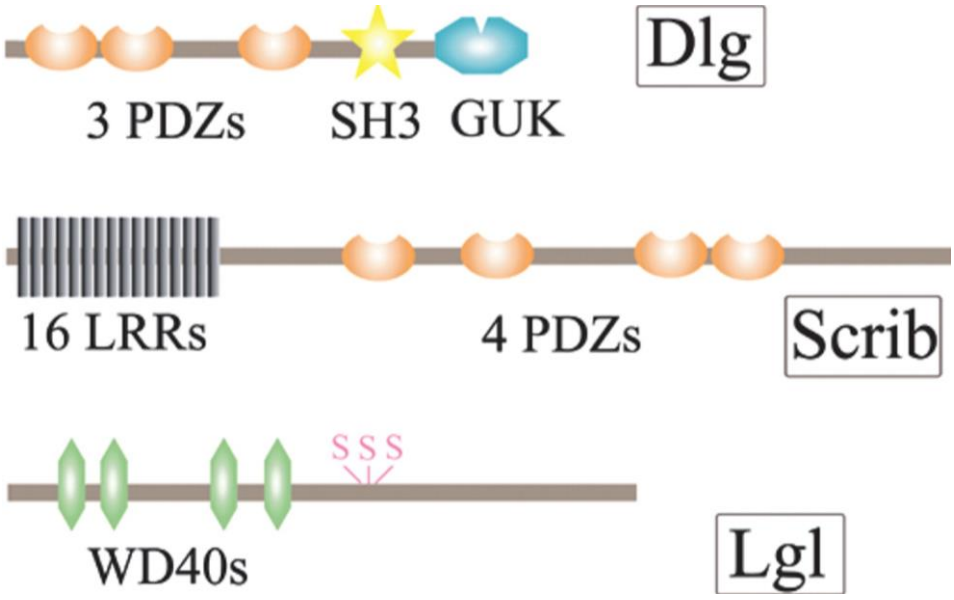

Figure 7. **Structure of Scribble complex proteins.** Disc large (Dlg) is a MAGUK (membrane-associated guanylate kinase) family protein, consisting of three PDZ domains, a SH3 (Src homology 3) domain, and a GUK (guanylate kinase-like) domain. Scribble (Scrib) is a LAP (LRR and PDZ) family protein, consisting of 16 LRRs (leucine-rich repeats) and 4 PDZ domains. Lethal giant larvae (Lgl) consists of tryptophan–aspartic acid 40 residue repeats (WD40s) and serine (S) residues that are conserved phosphorylation sites, which are targeted by aPKC. Adapted from Bilder, (2004).

Previous studies have provided solid evidence of Scrib, Dlg, and Lgl acting in a common pathway and through that regulating cell architecture, cell proliferation, and cell polarity (Bilder et al., 2000).

1.4 *Drosophila melanogaster* as a model organism to study cancer

Uncontrolled proliferation is the hallmark of cancer cells, and it is caused by defects in cellular growth signals, apoptosis, and alterations in metabolic pathways (Mirzoyan et al., 2019). Usually, epithelial cell function is monitored, and the cells that do not function properly are eliminated. But sometimes some of those cells can evade these control mechanisms, therefore forming tumours (Vidal & Cagan, 2006). The overproliferation of cancer cells is caused by several factors: proto-oncogenes (e.g., the RAS/RAF/MAPK axis) that induce activation of growth signals, inactivation of tumour suppressor genes, evasion of apoptosis, and reactivation of telomerase. Tumour cells are also able to disrupt the apico-basal cell polarity, which is associated with downregulation of cell-cell adhesion molecules and release of lytic enzymes (e.g., metalloproteases). These enzymes cause the degradation of the ECM, thereby allowing the cancer cells to invade and migrate to other tissues (Mirzoyan et al., 2019).

As flies have conserved signalling pathways that control cell growth and invasion similar to those in mammals, *Drosophila* serves as an excellent model for studying tumour biology. With genetic screens and different recombination techniques, it is possible to characterize the primary functions of conserved oncogenes and tumour suppressor genes within a whole organism. It is also possible to investigate the mechanisms of cellular growth of epithelial tumours in *Drosophila* larval imaginal discs (Mirzoyan et al., 2019). *Drosophila* is also a good model for studying tumour biology due to the possibility of forming tumours through single-gene mutations, in contrast with mammalian tumours that require a series of mutations to develop (Wodarz & Näthke, 2007).

Three ways to study human diseases using *Drosophila* model have been developed over the years. These strategies are reverse genetics, forward genetics, and a strategy to aid in the discovery of human disease-causing genes. The latter is also called the diagnostic strategy. Reverse genetics is used for studying the phenotype of human gene homologs in flies by creating mutations in these genes in flies. Forward genetics is used by inducing (e.g., chemically) mutations randomly, and later screening the animals for a particular phenotype. The diagnostic strategy gives an opportunity to assess the pathogenic properties of rare variants of genes linked to human disease through *Drosophila* (Ugur et al., 2016).

The various research and results provided by the fly community, and the model organism database for *Drosophila* – the FlyBase, which provides an online resource about genetic information, including complementary DNA (cDNA) resource, RNA interference (RNAi)

collections, etc., have also made it easier to research human disease through *Drosophila* (Millburn et al., 2016; Ugur et al., 2016).

1.4.1 Ras oncogene

The Ras family genes are among the earliest discovered oncogenes, and are described as proto-oncogenes, which play a crucial role in cell-cycle progression, metabolism, migration, cell survival, cell proliferation and differentiation (Gimple & Wang, 2019; Halfar et al., 2001). In mammalian cells, RAS is activated in response to mitogenic signals, and its activation is controlled by a highly conserved signalling pathway. This pathway is triggered by various cellular receptors, such as receptor tyrosine kinases (RTKs), G-protein coupled receptors (GPCRs), and integrin family members (Gimple & Wang, 2019; Halfar et al., 2001; Karim & Rubin, 1998). RAS is converted from an inactive GDP-bound form into an active GTP-bound form through the action of several scaffolding proteins assembled by these signalling pathways. Thus, acting as a molecular switch, RAS facilitates a variety of signal transduction pathways to send signals from the cell surface receptors, e.g., RTKs, to signalling molecules within the cell, e.g., mitogen-activated protein kinase (MAPK), promoting cell proliferation (Gimple & Wang, 2019; Prober & Edgar, 2000). According to The Cancer Genome Atlas (TCGA) project RAS pathway is the most frequently altered oncogenic pathway in cancer. Furthermore, mutations in *ras* genes contribute to about 20–30% of all human cancers (Gimple & Wang, 2019).

There are three *ras* genes in mammals: *K-ras, N-ras, and H-ras* (Karim & Rubin, 1998). Mutations in these genes have been associated with several diseases, such as melanomas or pancreatic adenocarcinomas (Gimple & Wang, 2019). Mammalian Ras oncogenes have three homologs in *Drosophila*: Ras1 (also known as Ras85D), Ras2, *and* Ras3. Among these, Ras1 is the most homologous to mammalian RAS, with about 75% sequence similarity (Prober & Edgar, 2000; Salzberg et al., 1993). Like in mammals, the Ras pathway serves multiple functions in *Drosophila*, including the specification of larval head and tail structures, controlling the signalling of the Torso RTKs, specification of ventral ectoderm fate in the embryo and dorsoventral polarity in the egg shell, and regulating cell growth and differentiation of wing veins and photoreceptor cells in imaginal discs (Halfar et al., 2001).

The constitutively activated form of the Ras oncoprotein is called Ras^{V12} (Zhang et al., 2024). This activating mutation was made in the *Drosophila Ras1* gene, where valine was substituted with glycine at residue 12 (Karim et al., 1996). The overexpression of Ras^{V12} causes benign tumor growth in *Drosophila*. For example, Ras^{V12} promotes cell growth in the wing imaginal

discs instead of the division of the cells. Ras^{V12} can be used as a model to identify pathways that are necessary for tumor development and metastasis (Miles et al., 2011; Prober & Edgar, 2000; Zhang et al., 2024). In previous studies, it has been implicated that the expression of Ras^{V12} under the control of the *sevenless* enhancer/promoter avoids the normal requirements for Sevenless RTK activity, and activates photoreceptor cell differentiation, therefore transforming the non-neuronal clone cells into disarranged photoreceptor cells (Fortini et al., 1992). In a research by Karim and Rubin (1998) it was indicated that the expression of $Ras^{V12,}$ under the control of the *eyeless* gene enhancer, causes overgrowth of both the eye-antennal imaginal discs and the adult eye, with the adult eye having a very irregular shape (Karim & Rubin, 1998).

1.4.2 Scribble mutants

There are several different Scrib protein mutations in *Drosophila*, a few of them are referred to as $Scrib^1$, $Scrib^2$, $Scrib^3$, $Scrib^4$, $Scrib^5$, $Scrib^6$, and $Scrib^7$ (Figure 8). These mutant proteins are caused by single base pair changes in the coding region of each *scrib* allele. Six of these changes generate premature stop codons, whereas $Scrib^1$ alters leucine 223, in LRR 10, to a glutamine, thus producing proteins with mutations in, or deletions of, many *scrib* interaction domains. Each mutant protein alters a stop codon in different regions of the protein. $scrib^2$ introduces a stop codon before the LRR domain, with the premature stop codon being generated in the third codon, whereas $scrib^3$ terminates within the LRR domain, specifically within the 12^{th} LRR. However, $scrib^4$, $scrib^5$, and $scrib^6$ alter the premature stop codons in the PDZ domains, with $scrib^4$ terminating amid PDZ1, $scrib^5$ terminating between PDZ2 and PDZ3, and $scrib^6$ terminating in the PDZ4 domain. $scrib^7$ generates a stop codon in the last part of the Scrib protein gene, removing the last 301 amino acids, without deleting any conserved domains (Zeitler et al., 2004).

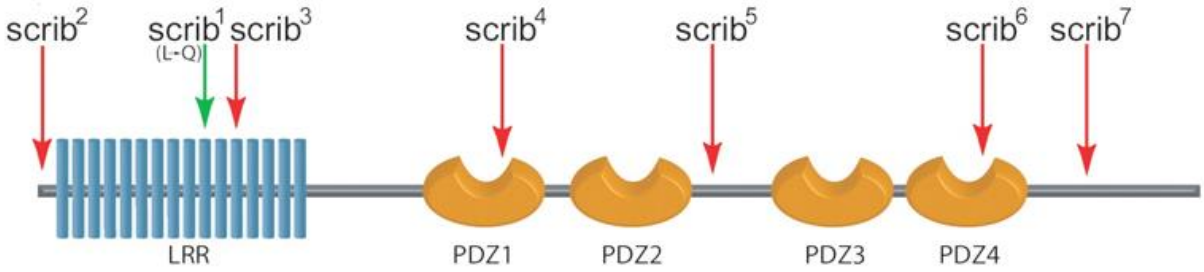

Figure 8. Locations of Scrib protein mutations. Single base pair changes mapped onto a diagram of a Scrib protein allele, where the red arrows indicate the locations of each mutant's premature stop codons, and the green arrow points to the location of a missense mutation. *scrib*^{2} has a termination codon in the third codon, cutting out most of the protein and its conserved domains. *scrib*^{3} terminates in the LRR domain, specifically in the 12th LRR. *scrib*^{4} has a premature termination codon within the PDZ1, whereas *scrib*^{5} has one in between PDZ2 and PDZ3, and *scrib*^{6} terminates in the PDZ4 domain. *scrib*^{7} terminates before the last 301 amino acids, without deleting any of the protein's conserved domains. In addition to the six premature termination codons, *scrib*^{1} has an alteration in the 10th LRR, altering leucine (L) 223 to a glutamine (Q). Adapted from Zeitler et al., (2004).

In a previous study by Zeitler et al. (2004), the *scrib* alleles 1, 2, and 3 were all indicated to have a lethal larval phase, whereas the alleles 4, 5, and 6 behave as hypomorphs, resulting in the organism dying in the early pupal stage. The *scrib*^{7} allele acts as a weak hypomorph; while hemizygous animals die during mid-pupal stages, homozygous animals die as pharate adults with normal external morphology. The *scrib*^{1}, *scrib*^{2}, and *scrib*^{3} mutant imaginal discs were found to have a rounded rather than elongated shape. The tissues exhibit an overproliferative phenotype, showing a drastic size difference compared to wild-type (WT) discs. The cells are multilayered, forming a solid spherical mass rather than a flat disc. In contrast, *scrib*^{4}, *scrib*^{5}, *scrib*^{6}, and *scrib*^{7} maintain the organized monolayered epithelia and the distinctive folded structure of the imaginal discs. *Scrib*^{4} and *scrib*^{5} show altered epithelial cell shapes and an intermediate size difference compared to WT discs, while *scrib*^{6} and *scrib*^{7} imaginal discs do not exhibit a substantial difference in tissue size compared to the WT discs. These results suggest that the LRR domain in Scrib protein is essential for maintaining cell polarization and regulating cell proliferation, while the PDZ domains are crucial for contributing to Scrib function in controlling cell polarity and proliferation (Zeitler et al., 2004).

The hypomorphic *scrib* allele, *scrib*^{5}, seems to be able to maintain ABP but has an overproliferated phenotype in imaginal discs. This indicates that the N-terminal LRR domain might be enough to maintain ABP, but not for growth control (Zeitler et al., 2004). In another study by Huang et al. (2023), this was further examined by comparing Scrib^{5} with Scrib^{2} using clonal analysis through mosaic analyses with a repressible cell marker (MARCM) system

(system further described in chapter 1.5.3). In wing imaginal discs containing null mutant clones (*scrib*^{2}), very small clones were produced, which also showed an autonomous reduction in the expression of atypical proteinase C (aPKC), an apical marker, and Dlg. In contrast, *scrib*^{5} clones did not show significant changes in aPKC and Dlg spatial distribution, suggesting that when *scrib*^{5} cells are surrounded by wild-type (WT) cells, Scrib^{5} protein is sufficient for maintaining ABP in the epithelial cells of wing imaginal discs. However, when *scrib*^{5} mutations affect the entire tissue, the animals exhibit overproliferated phenotypes along with a loss of apico-basal polarity. This indicates that in *scrib*^{5} tissues, ABP is not properly maintained, resulting in defective growth control, and suggests that *scrib*^{5} cells by themselves are incompetent in maintaining ABP, making them primed for malignancy. These results suggest that the behaviour of *scrib*^{5} mutant cells varies in a context-dependent manner (Huang et al., 2023).

1.4.3. Cooperation between Ras^{V12} and Scrib^{-}

Several studies have explored how the mutated oncogene *Ras*^{V12} and loss of *scrib*, the *scrib* null (*scrib*$^{-}$) allele (indicating either *scrib*^{1} or *scrib*^{2}), cooperate in tumorigenesis in *Drosophila*.

One of the studies by Brumby and Richardson (2003) shows that *Ras*^{V12} and *scrib*$^{-}$ (*scrib*^{1} allele) cooperate synergistically in the eye-antennal imaginal discs. While the eye-antennal disc tissues with *scrib*$^{-}$ mutatant clonal cells indicate loss in cell polarity, defective differentiation, and cell overproliferation, the tissue overgrowth appears to be restrained by apoptosis. But when ectopically activated Ras oncogene (Ras^{V12}) was expressed in *scrib*$^{-}$ clones, the tissues showed a drastic overproliferation, while also failing to differentiate, and continued to grow, showing a drastic difference in size compared to WT eye-antennal imaginal discs. In this genotype, the eye-antennal imaginal discs exhibit metastasis involving the brain lobes and other imaginal discs. The cooperation of these mutations also resulted in either lethal larval or pupal phases (Brumby & Richardson, 2003).

1.5 Genetic toolkit for the *Drosophila* model

1.5.1 Genetic mosaicism and clonal analysis

Genetic mosaicism has become a vital tool in *Drosophila* research, in the study of development and genetics, and the techniques of genetic mosaics induce mutations in a portion of cells or tissues in an individual organism (Blair, 2003; Germani et al., 2018). Individuals composed of cells with at least two different genotypes are called genetic mosaics, and usually, for mosaic analysis, homozygous mutant cells need to be generated from heterozygous precursors via mitotic recombination (Germani et al., 2018; Lee & Luo, 2001). Mosaic analysis makes it possible to examine mutant phenotypes, that would usually be lethal if applied to the entire organism, through the knock out of a gene function in some cells, and later examining their phenotypes in an otherwise phenotypically wild-type organism (Blair, 2003; Lee & Luo, 2001). For example, by limiting a mutation, that completely or partially removes the function of a given gene, to only a small number of cells, lethality in early development can be avoided, thus making it possible to examine the mechanisms of these mutant cells (Blair, 2003).

Genetic mosaics can occur naturally or be artificially induced. Mosaics can naturally occur due to inaccurate repair of DNA double-strand breaks by homology-directed repair (HDR), or due to ionizing radiation causing ring-X chromosomes, where the two of the X chromosome arms have fused together, forming a ring (Germani et al., 2018). There are also several ways to induce genetic mosaics. There are more classical ways, including surgical approaches, chromosome loss, and mitotic recombination, and additional, more improved techniques, such as FLPase recombination target (FRT)-mediated mitotic recombination, or the Gal4-UAS system (Blair, 2003).

Surgical approaches are the oldest of the three classical techniques, and usually involve either transplanting cells, nuclei, or whole tissues (e.g., imaginal discs) between different fly strains. Due to difficulties in analysing the transplanted tissues due to their size or faulty differentiation, chromosome loss, and mitotic recombination are mainly used for creating mosaics in flies (Blair, 2003).

Loss of the three autosomes, the X chromosome, or the Y chromosome during the development of the fly's embryo can be induced by several mutations (Blair, 2003). For example, gynandromorphs are mosaics that consist of male and female parts, which is caused by the mitotic loss of one X chromosome during embryonic development (Germani et al., 2018).

Finally, the mitotic recombination between the arms of homologous chromosomes is used. This can occur spontaneously in flies but can be induced by X-rays or γ-rays. Due to induced mitotic recombination, the homozygous daughter cell almost always forms a single clone that differs from the original, these clones can later be examined and analysed (Blair, 2003). For clonal analysis, in various imaginal disc tissues, these mutant clone cells need to be marked by nonlethal, and easily detectable cell markers, such as the *white* (w) gene as the eye marker, which together with the wild type red pigment produces red and white patches in the adult *Drosophila* eyes, and green fluorescent protein (GFP). (Germani et al., 2018).

1.5.2 FLP and Gal4-UAS system

The flippase (FLP)/FRT recombination system is used for generating mosaics through site-specific recombination between homologous chromosomes. FLP is a site-specific recombinase (FLPase) that recognizes FLPase recombination targets (FRTs), thus catalysing cleavage and chromosomal exchange (Blair, 2003; Germani et al., 2018). There are two ways to use FLP/FRT system, one of which is FRT-mediated mitotic recombination, and the other is FRT-mediated FLPout constructs. The FRT-mediated mitotic recombination uses two FRT sites that are inserted into homologous chromosomes, and FLP, which is activated, e.g., through heat shock, recognizes the FRT sites and causes recombination between them. While the FRT-mediated FLPout constructs also have two FRT sites and an FLP, the FRT sites of this construct are on the same chromosome and are used for removing part of the DNA that is between the FRT sites (Blair, 2003).

To increase the rate of recombination with FLP, the Gal4 (yeast transcriptional activator protein)/UAS (upstream activating sequence) system can be used (Blair, 2003). The Gal4/UAS system allows for insertion of any gene of interest into the genome through Gal4 protein binding to the UAS sequence. For example, Gal4 can be used to express mutant proteins from other species in *Drosophila* to generate phenotypes for genetic screens. Gal4 is an activator from yeast and can activate transcription in flies via promoters bearing Gal4 binding sites (Brand & Perrimon, 1993). In the system, there are two transgenes, from which the first contains cDNA of interest connected to the UAS sequence, which is the binding site for the Gal4 transcription activator. The second contains the Gal4 coding region, which is under the control of a spatially delimited enhancer. The target gene, controlled by the UAS sequence, is activated when the two transgenes are brought together and Gal4 is made in a spatially-determined pattern, which in turn is dependent on the activation of the enhancer (Stebbins & Yin, 2001).

1.5.3 The MARCM system

The mosaic analyses with a repressible cell marker (MARCM) system is essential for mosaic analysis and makes it possible to uniquely label homozygous mutant cells in mosaic tissues. The mutant cells are induced with the MARCM system by using Gal80, which is also a yeast protein, together with the Gal4/UAS system. Normally Gal80 protein inhibits the activity of Gal4 transcription activator, but after the FLP/FRT-mediated mitotic recombination, the transgene containing Gal80 is removed, thus allowing the expression of the Gal4-dependent reporter gene (Lee & Luo, 2001). The MARCM system is used to mark specific clone cells of a recombination event while leaving the non-clonal cells unmarked (Germani et al., 2018).

The MARCM system typically consists of flies carrying a FLP, a transgene containing Gal4, which is driven by a promoter (e.g., actin), a UAS-GFP (or any other fluorescent marker) marker, and FRT sites that are heterozygous for a mutation in the gene of interest. UAS-GFP expression in a clone cell is determined by the continuously expressed Gal80 that is positioned distal to one of the FRT sites. When FLP is expressed, the two FRT chromosomes recombine, generating two different daughter cells via chromosomal segregation. One daughter cell has two copies of Gal80 expressed, which inhibits Gal4 activity and therefore keeps the cell unmarked. The second daughter cell does not express Gal80, which allows Gal4 to activate, thus activating the expression of UAS-GFP and marking the cell (Germani et al., 2018).

2. EXPERIMENTAL PART

2.1 Aims of the thesis

The mutated Scrib^{5} protein (*scrib^{5}* allele) appears to behave in a context-dependent manner. When Scrib^{5} mutant clones are surrounded by wild-type cells, it seems sufficient for controlling apico-basal polarity (ABP) and cell proliferation. However, when *scrib^{5}* is expressed in the whole tissue, the tissues exhibit a loss of ABP and an extreme overproliferative phenotype (Huang et al., 2023).

It was hypothesized for this thesis that when the constitutively activated proto-oncogene *Ras^{V12}* and the mutated neoplastic tumour suppressor gene *scrib^{5}* are expressed together, the Scrib^{5} protein is not able to maintain ABP, causing severe overproliferation of the eye-antennal imaginal disc tissues, similar to the Scrib^{5} expression in the whole tissue, and the synergies between oncogene expression, such as Ras, and the loss of tumour suppressor genes.

A hypothesis was put forward:

- Mutated tumour suppressor Scrib^{5} might cooperate synergistically with activated proto-oncogene Ras^{V12} when expressed together, resulting in eye-antennal imaginal disc tissues losing ABP, and therefore forming an overproliferated, tumour-like structure.

The aims of this thesis are:

1. To elucidate whether the *scrib^{5}* allele can maintain ABP when expressed together with activated oncogene Ras^{V12},
2. To unveil whether Ras^{V12} and Scrib^{5} synergize and cooperate when expressed together, forming a stronger tumour-like phenotype compared to Ras^{V12} mutant individually in the eye-antennal imaginal discs.

2.2 Materials and methods

2.2.1 Fly stocks

All fly stocks utilized in the experiments for this thesis were either available in the host lab or obtained from the stock centers, e.g., Bloomington Drosophila Stock Center (BDSC – (Bloomington Drosophila Stock Center, 2021)). The fly lines used in this thesis are listed in Table 1.

Table 1. Fly lines utilized in the thesis

Genotype of the fly line	Line number in Bloomington	Purpose
eyFlp; AyGal4, UAS-GFP/CyO; FRT^{82B}-Gal80	N/A	Generating mutant clones via the MARCM system. For all crosses, female flies used for crosses were from this stock. #305, host lab stock
w[1118]; P{ry[+t7.2]=neoFRT}82B P{w[+mC]=Ubi-GFP(S65T)nls}3R/TM6B, Tb[1]	32655	For negative control, to determine clone cell size, male flies from this stock were used for the cross. #674
FRT^{82B}; $scrib^{2}$/Tm6B	N/A	For the *$scrib^{2}$* mutant clone generation, male flies from this stock were used for the cross. #61, host lab stock
FRT^{82B}; $scrib^{5}$/Tm6c	N/A	For the *$scrib^{5}$* mutant clone generation, male flies from this stock were used for the cross. #128, host lab stock
UAS-Ras^{V12}/CyO; FRT^{82B}/TM3TbSb	N/A	For the *Ras^{V12}* ectopic expression, male flies from this stock were used for the cross. Fly line generated in the host lab
UAS-$Ras85D^{V12}$/CyO; FRT^{82B}-$scrib^{2}$/TM6TbSb	N/A	For the *Ras^{V12}* and *$scrib^{2}$* combination mutant clone generation, male flies from this stock were used for the cross. Fly line generated in the host lab

UAS-Ras85D^{V12}/CyO; FRT^{82B}-scrib^{5}/TM6TbSb	N/A	For the *Ras^{V12}* and *scrib^{5}* combination mutant clone generation, male flies from this stock were used for the cross. Fly line generated in the host lab

2.2.2 Husbandry of flies

The flies were kept in plastic vials containing 12 ml of fly food at the bottom of the vial. The food for the flies contains eight main ingredients: water, corn flour, soy flour, glycose, sucrose, sugar syrup, yeast, and agar. 15 ml of propionic acid and 30 ml of Nipagin were added to the food to prevent spoilage and mold growth.

Vials containing flies were typically kept in an 18 °C incubator (PHCbi), but when generating the mutant genotypes, the crosses were kept in a 25 °C incubator (PHCbi). This was necessary since the *Gal4* and *Gal80* are heat-sensitive alleles (Matsumoto et al., 1978).

When crossing flies, 25 female and 20 male flies were generally used for each cross.

2.2.3 Mutant clone generation

In the given thesis, the MARCM system was selected for the experiments to generate mutant clone cells in the eye-antennal imaginal discs, marked with GFP, thus allowing for imaging and analysis of the tissues. Female flies for the crosses were obtained from the stock containing necessary components, like the Gal4/UAS system, Gal80 protein, FLP, and FRT, for generating the clone cells with the MARCM system. For the clone cell generation, the other fly lines used for crosses had to also contain a FRT site, for the FLP/FRT-mediated mitotic recombination, thus removing the transgene containing Gal80 protein and allowing for the GFP expression in the daughter cells (the clone cells).

2.2.4 Crosses

Six different crosses were made for the experiments.

First cross for negative control:

- ♀ *eyFlp;(AyGal4, UAS-GFP)/CyO; FRT^{82B}-Gal80* X ♂ #674: *FRT^{82B}; ubi>GFP (nls)*

Second cross for *scribble^{2}* clone cells in larvae' eye-antennal imaginal discs:

- ♀ *eyFlp;(AyGal4, UAS-GFP)/CyO; FRT^{82B}-Gal80* X ♂ #61: *FRT^{82B}; scrib^{2}/Tm6B*

Third cross for *scribble^{5}* clone cells in larvae' eye-antennal imaginal discs:

- ♀ *eyFlp;(AyGal4, UAS-GFP)/CyO; FRT^{82B}-Gal80* X ♂ #128: *FRT^{82B}; scrib^{5}/Tm6c*

Fourth cross for *Ras^{V12}* clone cells in larvae' eye-antennal imaginal discs:

- ♀ *eyFlp;(AyGal4, UAS-GFP)/CyO; FRT^{82B}-Gal80* X ♂ *UAS-Ras^{V12}/CyO; FRT^{82B}/Tm3TbSb*

Fifth cross for *Ras^{V12}/scribble^{2}* clone cells in larvae' eye-antennal imaginal discs:

- ♀ *eyFlp;(AyGal4, UAS-GFP)/CyO; FRT^{82B}-Gal80* X ♂ *UAS-Ras85D^{V12}/CyO; FRT-scrib^{2}/Tm6TbSb*

Sixth cross for *Ras^{V12}/scribble^{5}* clone cells in larvae' eye-antennal imaginal discs:

- ♀ *eyFlp;(AyGal4, UAS-GFP)/CyO; FRT^{82B}-Gal80* X ♂ *UAS-Ras85D^{V12}/CyO; FRT^{82B}-scrib^{5}/Tm6TbSb*

2.2.5 Picking up larvae and dissection

After crossing to obtain the wanted samples, the third instar larvae were collected from the side of the vial. To obtain the larvae with genetic mosaics of *scrib^{2}*, *scrib^{5}*, *Ras^{V12}*, *Ras^{V12}/scrib^{2}*, or *Ras^{V12}/scrib^{5}*, individuals displaying the non-tubby (Tb – short body) phenotype, characterized by normal body size, were collected. The collected larvae were put in a 6-well dish containing 1x phosphate-buffered saline (PBS), and each genotype of larvae was put in a separate well. The larvae were immobilized by keeping the dish with the larvae on ice. After collecting the larvae, they were examined under a Leica M165 FA fluorescent stereo microscope equipped with a Leica DFC450 C camera to determine whether the larvae were expressing the GFP signal

(Figure 9B–F). The larvae positive for the GFP signal were with the desired genotypes, e.g., negative control or Ras^{V12}.

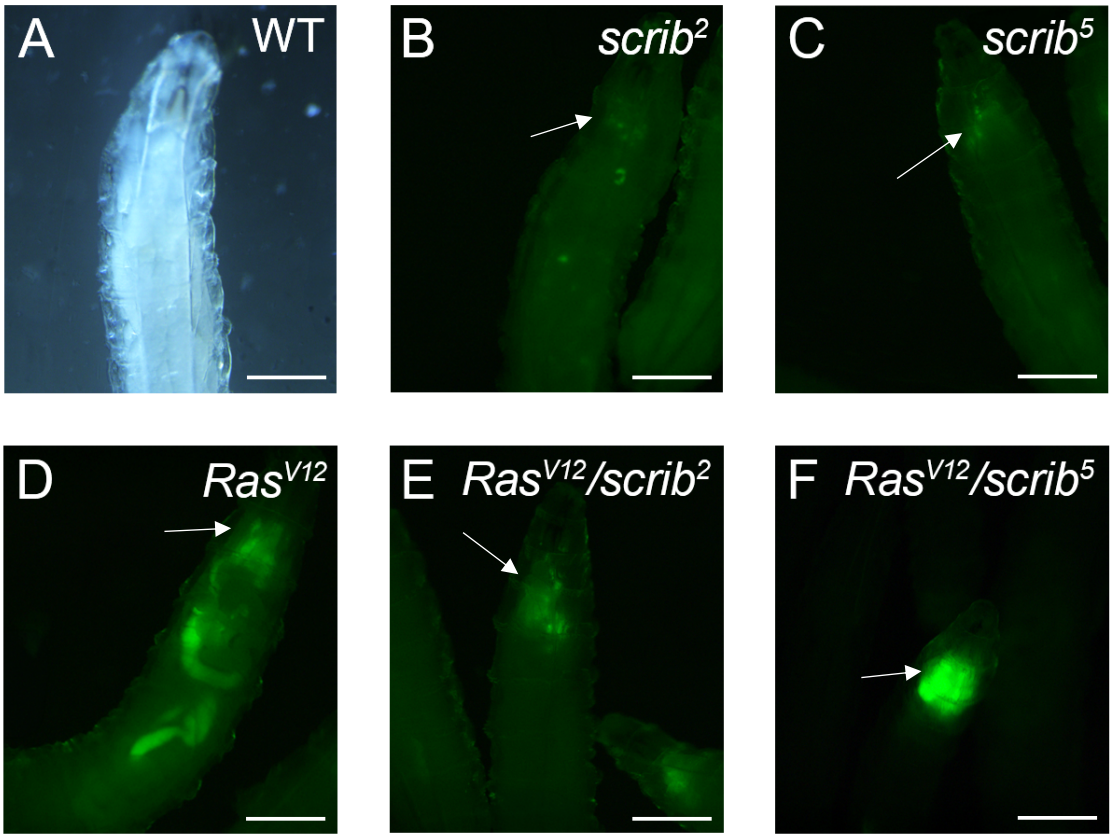

Figure 9. Identification of mutant cell clones in the eye-antennal imaginal discs of larvae. The presence of mutant cell clones was identified using epifluorescence microscopy and a fluorescent marker (GFP). The different mutant clones show different GFP signal intensities. (A) Wild-type (WT) larva for comparison. (B-F) Fluorescent (GFP signal) of *scrib*^{2} (B), *scrib*^{5}(C), *Ras*^{V12} (D), *Ras*^{V12}/*scrib*^{2} (E), and *Ras*^{V12}/*scrib*^{5} (F) mutant clones in the larval eye-antennal imaginal discs. Arrows indicate the position of eye-antennal imaginal discs. Scale bars: 500 µm.

After picking out the GFP-positive larvae, they were dissected to isolate the imaginal discs. For dissection, a Zeiss Stemi 305 stereo microscope, a clean silicone pad, 1x PBS, and forceps were used. The clean silicone pad was placed under the microscope, about 50 µl of 1x PBS was added onto the pad, and a larva was placed on the pad into the PBS. Then, in order to get the tissues out of the larva, the larva was grabbed from the posterior part with one pair of forceps, and just behind the mouth part with the second pair of forceps, which were then used to slowly and carefully pull from the mouth part. Due to that, the outer shell of the larva would break and expose the insides of the larva. Then all the unnecessary parts, such as the posterior part of the larva and the intestines, were removed, leaving behind only the mouth part, the brain, and the

imaginal discs, including the pair of eye-antennal imaginal discs attached to the brain. The dissected tissues were put in a four-well dish containing 450 µl of PBS, and tissues with each genotype were put in separate wells.

This sample collecting process was repeated about 15 times to obtain enough tissues for analysis.

2.2.6 Fixing tissues

After dissection, the tissues were fixed in 3.7% Formaldehyde (FA)- phosphate-buffered saline (PBS) solution in a four-well dish at room temperature (RT) for 20 minutes. 37% FA solution was diluted (1:10) in PBS solution and added to the dissected tissues for fixation.

After fixation, the fixative was carefully removed from the tissues under a Zeiss Stemi 305 stereo microscope. The tissues were then washed with PBS solution containing 0.1% Tween-20 (PBT) five times with gentle stirring. First, the first two times, 400 µl of PBT was added to the tissues for a brief rinse, and the solution was then removed under a microscope, to make sure not to remove any of the tissues from the dish. The next three washes were performed similarly, except that the tissues were kept in the washing solution for five minutes each. After washing, the tissues were covered with 400 µl of PBT, and either kept in a +4 °C fridge or used for the staining.

2.2.7 Staining tissues

In this thesis project, two different types of staining were used. The first involved staining for actin and DNA, using Phalloidin (Phalloidin-AlexaFluor 568; Thermo Fisher Scientific) and DAPI (4',6-diamidino-2-phenylindole; Thermo Fisher Scientific), respectively. The second staining was for basolateral polarity marker Discs large 1 (Dlg; Developmental Studies Hybridoma Bank - DSHB) and DNA staining, using mouse monoclonal 4F3 anti-disc large (Dlg) antibody and DAPI, respectively.

For the first staining process, the mixture of PBT, DAPI, and Phalloidin 568 was made. This staining method was used for determining the differentiation and proliferation in the eye-antennal imaginal disc cells, and how the developing eye pattern is formed. 1000 µl of PBT was mixed with 1 µl of DAPI (dilution of 1:1000) and 1 µl of Phalloidin 568 (dilution of 1:1000) and then divided equally between the four wells of the dish. The tissues were kept in the solution

for the staining process at RT, protected from light for two hours, after which the tissues were washed with PBT five to six times, similarly to the washing after the fixation process, except the tissues were kept in PBT for 10 minutes. The tissues were kept in 400 µl of PBT and used for making slides for imaging.

For the second staining, in addition to DAPI, mouse monoclonal 4F3 Dlg primary antibody (DSHB) and goat anti-mouse IgG H&L (Alexa Fluor 568) secondary antibody (Abcam) were used, which can be obtained from the Developmental Studies Hybridoma Bank (DSHB) and Abcam. This staining method was carried out to determine polarity in the eye disc epithelial cells. After fixation and washing, the tissues were first blocked with 5% Normal Goat Serum (NGS; Thermo Fisher Scientific) for one hour at RT to reduce nonspecific background and therefore increase image quality (Proteintech Group, 2002-2025). After blocking, the mouse anti-Dlg antibodies were diluted 1:40 in 350 µl of 5% NGS blocking solution on the tissues, and the tissues were kept in the NGS-antibody mixture at +4 °C overnight. On the next day, the tissues were washed with PBT, similarly to the washing after fixation, and then the secondary antibody was added. The secondary antibody, Goat anti-mouse (Alexa Fluor 568) solution, was diluted 1:200 in PBT solution, and then added to the tissues. The tissues were kept in the mixture at RT for two hours, after which the tissues were again washed with PBT. The tissues were briefly rinsed twice with 400 µl of PBT and then washed once for five minutes with 400 µl of PBT. After washing, DAPI solution (1:1000 dilution in PBT) was added to the tissues, about 250 µl into each well, and kept on them for 30 minutes at RT, protected from light. After 30 minutes, the DAPI solution was removed, and the washing was continued, with the tissues washed three times with PBT for five minutes each time. After washing, the tissues were ready to use for making slides for imaging.

2.2.8 Tissue mounting and slide preparation

For mounting tissues on the slide glass, the following objects were necessary: slide glasses, cover glasses, VECTASHIELD Antifade Mounting Medium (Vector Laboratories), and clear nail polish.

As only the eye-antennal imaginal discs were necessary for the analysis, the previously fixed and stained tissues were further dissected. For the dissection, the Zeiss Stemi 305 stereo microscope with 4.0x zoom was used, a silicone pad was placed under the microscope, about 20 µl of PBS was added onto the silicone pad, and one of the previously fixed and stained tissues was placed in the PBS. Then the slide glass was prepared for mounting. On the slide

glass, 10 µl of the VECTASHIELD Antifade mounting medium was added, which was used to avoid the fading of the fluorescence signal, into which, after dissection, the imaginal discs were placed.

For separating the eye-antennal imaginal discs from the brain and the mouth part, a method of slowly pulling the mouth part with the forceps while with the other pair of forceps holding the brain still was used. With this method, the eye-antennal discs were separated from the brain lobes, after which it was easier to detect the connection between the eye discs and the mouth part, and cut it using the forceps, separating the eye discs from the mouth part. Another method was also used, when the mouth part was separated from the eye-antennal discs first, then the connection between the brain lobes and the eye discs had to be detected and cut using the forceps.

After the pair of eye-antennal imaginal discs was separated from the brain and the mouth, they were placed into the mounting medium on the slide glass. Then, more discs were separated, so about 6-8 discs would be mounted on one slide glass. After enough of the eye-antennal discs were separated and mounted on the slide glass, a cover glass was put on top of the slide glass, and something was added on one side of the cover glass for weight to make the tissues flatter. When the mounting medium had spread evenly under the cover glass, the edges of the cover glass were covered with clear nail polish to avoid drying of the sample.

The slide preparation process was repeated 4 times with each genotype of eye-antennal imaginal discs separately.

2.2.9 Microscopy

Three different microscopes were used for different parts of the experiments. The Leica M165 FC fluorescent stereo microscope equipped with a Leica DFC450 C camera was used for detecting the GFP signal in collected larvae with different genotypes. The Zeiss Stemi 305 stereo microscope was used for the dissections, and when washing the tissues, to avoid removing any tissues from the dish with the pipette. Finally, the Olympus FluoView 1000 confocal microscope was used for imaging of the samples, using the 60x objective.

2.2.10 Image analysis

The obtained images were viewed, analysed, and adjusted using the 3D image analysis software Imaris Viewer and ImageJ/FIJI. The Imaris File Converter program was also used for converting the image files (.oib) obtained from the confocal microscope into the .ims format for viewing them in the Imaris Viewer.

Protocol for using ImageJ/FIJI: First, open the .oib file and then launch the FIJI program. From there, select File, then Import, and Bio-Formats, and choose the .oib file. The Bio-Formats Import Options will then appear on the screen; from there, select Hyperstack and check Split channels, then click OK. Once the image opens, you can use the Z-slider to navigate through the stack to determine the Z-slice range. After that, from the Image icon, select Stacks, then Tools, and Make Substack. Enter the Z-slice range to create the substack. With the substack selected, go to the Image icon, select Stacks, and then Z project. A dialog will open; from there, set the projection type to maximum intensity and click OK. Then, from the Image icon, choose Color and select Merge Channels. Assign each channel to the appropriate color and click OK. Finally, from the File icon, select Save As, choose the TIFF or other preferred format, and the image will be saved.

2.3 Results

Although the loss-of-function of tumour suppressor genes such as *scrib* has been widely discussed as playing a significant role in tissue homeostasis, previous in vivo analyses of mutant cells have shown that their behaviour can vary in a context-dependent manner. For example, null mutant clones of *scrib* (*scrib*^{2}) form only small clones due to cell competition mechanisms (Huang et al., 2023). In contrast, the hypomorphic *scrib5* mutant exhibits distinct behaviour (Zeitler et al., 2004). *scrib*^{5} mutant clones in the *Drosophila* wing imaginal discs are larger than those of *scrib* null mutants. Important, apico-basal polarity is largely restored when these mutant cells are surrounded by wild-type cells (Huang et al., 2023). Therefore, in this thesis project, we focus on evaluating different *scrib* mutant alleles using *Drosophila* larval eye-antenna discs as an excellent model for studying tissue homeostasis.

Previous studies have also shown that synergies between oncogene expression, such as Ras, and the loss of tumour suppressor genes lead to more aggressive neoplasia and metastasis (Brumby & Richardson, 2003). Therefore, my studies also include synergistic analysis using different alleles of *scrib* mutants, and the constitutively activated form of proto-oncogene Ras:

scrib^{2}; *scrib*^{5}; *Ras*^{V12}; *Ras*^{V12}/*scrib*^{2}; *Ras*^{V12}/*scrib*^{5} in the developing eye-antennae discs of *Drosophila*.

To investigate whether the crosses for genetic mosaic larvae were successful, the adult fly's phenotypes were analyzed. The eye phenotypes of *scrib*^{2} and *scrib*^{5} mutant clones were relatively mild, showing only minor alterations in the patterning of the ommatidia (Figure 10C–D; Appendix 1B). For *Ras*^{V12}, *Ras*^{V12}/*scrib*^{2}, and *Ras*^{V12}/*scrib*^{5} mutant clones, first, the viability of these flies was assessed. Previous studies have shown that animals with *Ras*^{V12} and *Ras*^{V12}/*scrib*^{2} mutant genotypes typically die during the larval or pupal stages (Brumby & Richardson, 2003). Interestingly, we observed that flies resulting from *Ras*^{V12}/*scrib*^{2} cross developed into adult flies but exhibited severely altered eye phenotypes (Figure 10B; Appendix 1C). This discrepancy may be due to differences in genetic background.

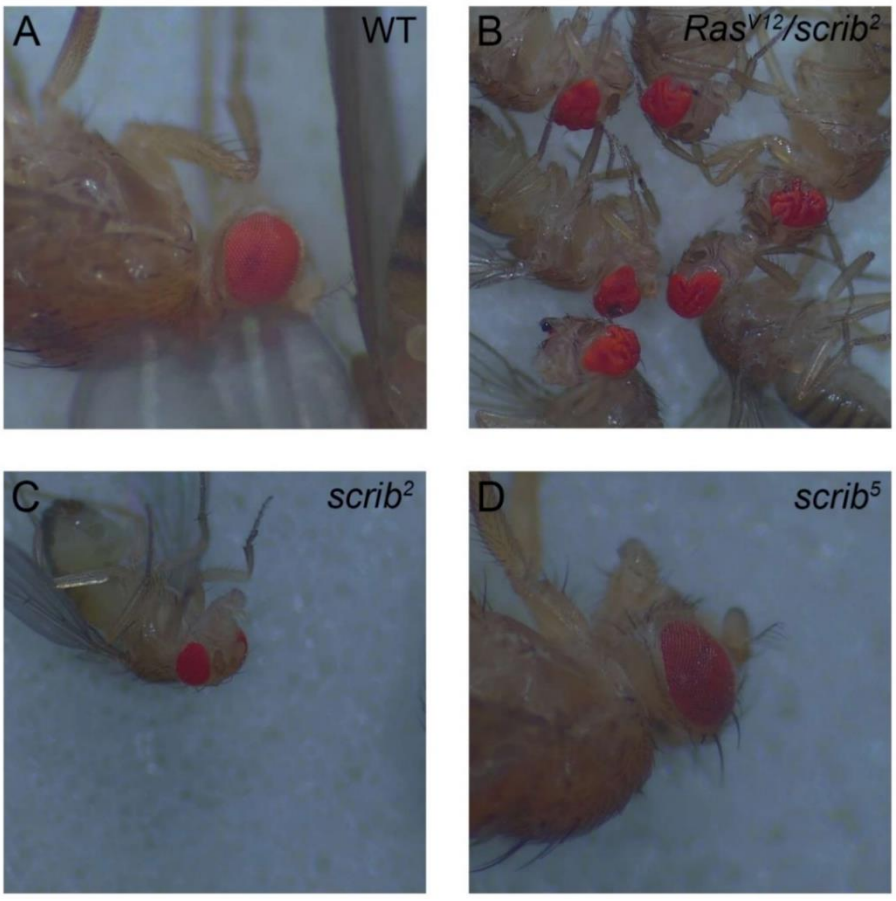

Figure 10. The adult fruit fly eyes phenotypes associated with different mutant clones. (A) Wild-type (WT) compound eye with regular patterning. (B) Severely affected eyes (mutant clones with *Ras*^{V12} and *scrib*^{2} together) exhibited strongly folded neoplastic phenotypes. (C, D) Milder phenotype of eyes (minor alterations in the patterning of ommatidia), with *scrib*^{2} (C) and *scrib*^{5} mutant clones (D).

2.3.1 Mutant clones in eye-antennal discs development

To understand how *scrib*^{2}, *scrib*^{5}, *Ras*^{V12}, *Ras*^{V12}/*scrib*^{2}, and *Ras*^{V12}/*scrib*^{5} mutant clones affect developing eye tissue development and homeostasis, the eye-antennal imaginal discs of larvae were examined. The discs were then stained and used for imaging. The tissues were stained with Phalloidin 568 (AleaFluor 568), which stains the actin filaments (F-actin) and emits red fluorescence when examined under a fluorescent microscope, and with DAPI (data not shown), which stains the DNA, therefore the entire nuclei, and emits blue fluorescence when examined under a fluorescent microscope. The Phalloidin 568 staining allows for visualization of the pattern and positioning of the developing future compound eye cells, the ommatidia, and the DNA staining with DAPI allows for examination of the positioning of the cells, indicating if the cells are monolayered or multilayered (data not shown).

Negative control was established for determining the size and patterning of the eye discs, and GFP-marked clone cell size in the tissues with the WT phenotype, and for comparison with the tissues containing clone cells with mutant phenotype. Phalloidin staining revealed normal patterning in the eye imaginal discs, including the morphogenetic furrow (MF) and differentiated pigment cell precursors (Figure 11A-A'').

The eye-antennal discs from the *scrib*^{5} genotype individual showed slightly smaller clone sizes compared to the negative control. Subtle changes are observed in eye patterning within regions containing clone cells, and the MF appears to be slightly irregularly aligned (Figure 11C-C'').

When analysing *scrib*^{2} tissues, the clone size appears significantly smaller compared to the negative control, consistent with previous reports that *scrib*^{2} mutant cells are efficiently eliminated through cell competition. The pattern of the future eye is mostly normal, and the MF is also regularly shaped. Still, there can be seen slight irregularities in the areas containing mutated clone cells, containing delamination cells (Figure 11B-B'').

Eye-antennal imaginal discs containing ectopically activated oncogene *Ras*^{V12} clone cells (Figure 11D-D'') show a more severe neoplastic phenotype and indicate tissue overgrowth compared to the negative control discs (Figure 11A-A''). The clone size is substantially larger, and the mutant cells have spread more extensively throughout the tissue. The patterning of the future eye and the MF is highly irregular, indicating disruptions in cell differentiation.

When analysing and comparing tissues expressing *Ras*^{V12} and *scrib*^{2} with negative control, the tissue shape and size appear highly irregular. Regions containing clones lose the future eye patterning (Figure 11E-E''). Clone cells are extensively migrated throughout the eye-antennal

disc and into the brain lobe (data not shown), suggesting a highly metastatic behaviour. Also, the MF is missing within the clone, indicating a failure in differentiation. The overall increase in tissue size reflects drastic overproliferation of disc cells, and the combination of Ras^{V12} and $Scrib^{2}$ appears to act synergistically to drive this phenotype.

Since the synergy between Ras^{V12} and $Scib^{5}$ has not been previously reported, the resulting phenotypes were carefully analysed. Eye-antennal imaginal discs expressing both Ras^{V12} and $Scrib^{5}$ protein (Figure 11F-F'') exhibited a drastically increased tissue size compared to negative control tissues (Figure 11A-A''). These tissues also appeared to form a multi-layered structure, more pronounced than in tissue expressing the Ras^{V12} clone. This indicates that the cooperative interaction between Ras^{V12} and $Scrib^{5}$ led to more severe overproliferation and significant loss of apico-basal polarity (ABP). These findings indicate that $Scrib^{5}$ protein may be insufficient to maintain ABP in the presence of oncogene co-expression, highlighting a cooperative molecular network between oncogenes and tumor suppressor genes under both physiological and pathological conditions. The future eye patterning was highly irregular, and only some irregular patterning could be seen in areas that do not contain mutant clone cells. These results indicate that Ras^{V12} and $Scrib^{5}$ synergize in the formation of significantly enlarged, overproliferated eye-antennal imaginal disc tissue.

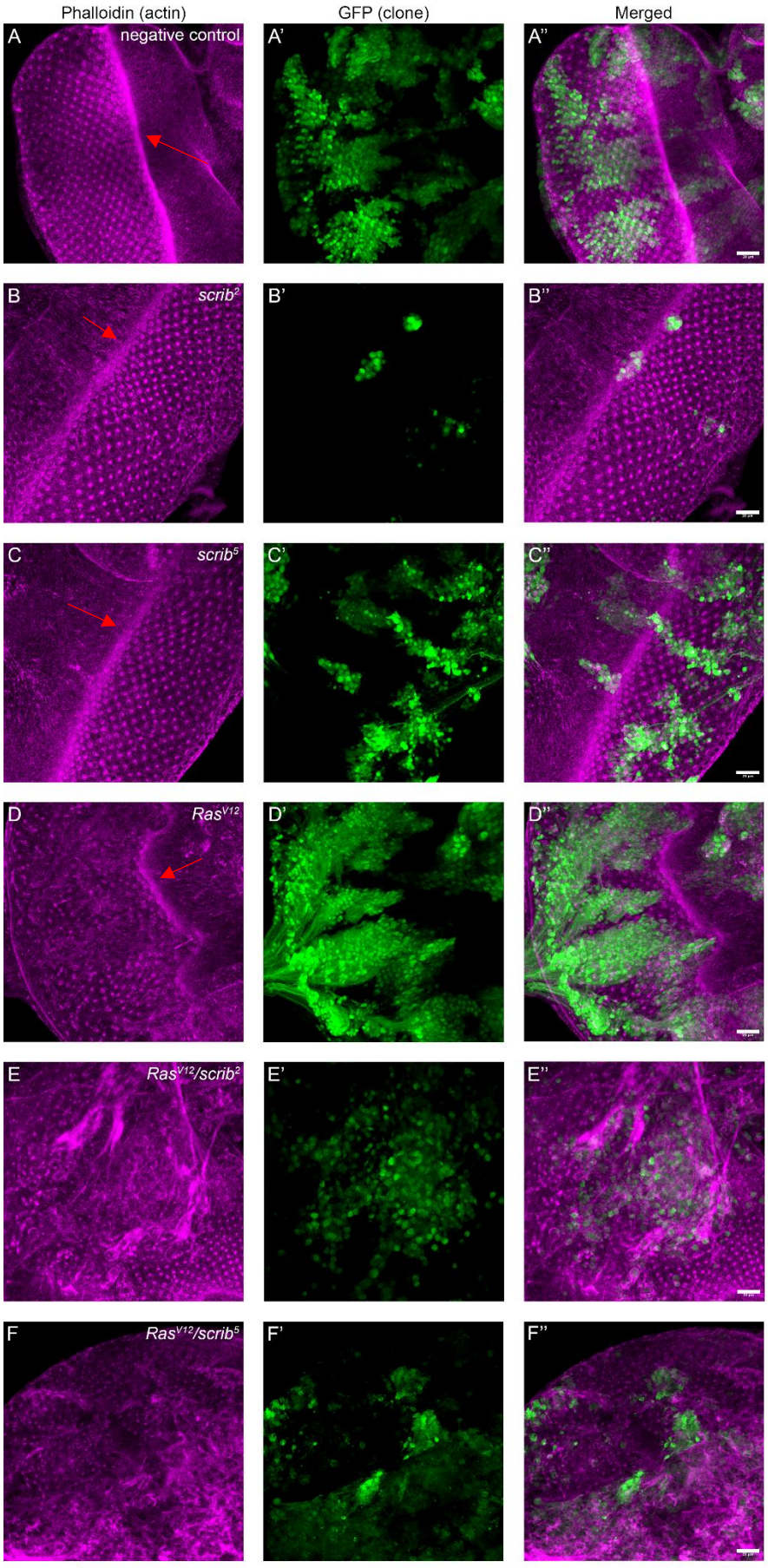

Figure 11. Image panels showing the future adult eye pattern of eye-antennal imaginal discs with different genotypes. Mutant clones visualized with GFP (green) signal and

Phalloidin (magenta) staining, indicating patterning of the future eye cells via actin filaments. Images were taken with the Olympus FluoView 1000 confocal microscope, using a 60x objective. The red arrows indicate the morphogenetic furrow in the tissues. (A–A'') Eye-antennal disc with control clones. (B–B'') *scrib*^{2}, (C–C'') *scrib*^{5}, (D–D'') *Ras*^{V12}, (E–E'') *Ras*^{V12}*/scrib*^{2}, (F–F'') *Ras*^{V12}*/scrib*^{5} mutant clones in the eye-antennal disc. Scale bars: 20 µm.

2.3.2 Ras^{V12}/Scrib^{5} tissues indicate loss of polarity

To investigate how *scrib*^{5} mutant cells maintain apico-basal polarity (ABP), the Dlg staining, a marker and key component of the baso-lateral polarity complex, was used to label the cellular membrane of epithelial cells in the eye-antennal imaginal discs (Dorot et al., 2017).

The tissues with negative control clones show a regular localization of Dlg protein at the cell membrane, indicating that the cells have established ABP and are properly positioned (Figure 12A–A'').

Next, the *scrib*^{5} clone cells marked by GFP expression were examined (Figure 12B–B''). Dlg staining revealed that Dlg localization was diffusely distributed within the Scrib5 mutant clones without noticeable disruptions in ABP. This suggests that Scrib5 may be sufficient to maintain ABP in the eye-antennal imaginal disc, even when mutant cells are surrounded by wild-type cells.

Significant changes in ABP were observed in *Ras*^{V12}*/scrib*^{5} clones. Tissues expressing both the oncogene Ras^{V12} and the mutated nTSG Scrib^{5} seem to have largely lost cell polarity across most parts of the eye-antennal disc (Figure 12GC–C''). These findings further support that the synergy between Ras^{V12} expression and Scrib^{5} mutations enhances neoplasia and metastasis of clone cells, likely due to the limited ability of Scrib^{5} to function as an ABP determinant (Figure 12).

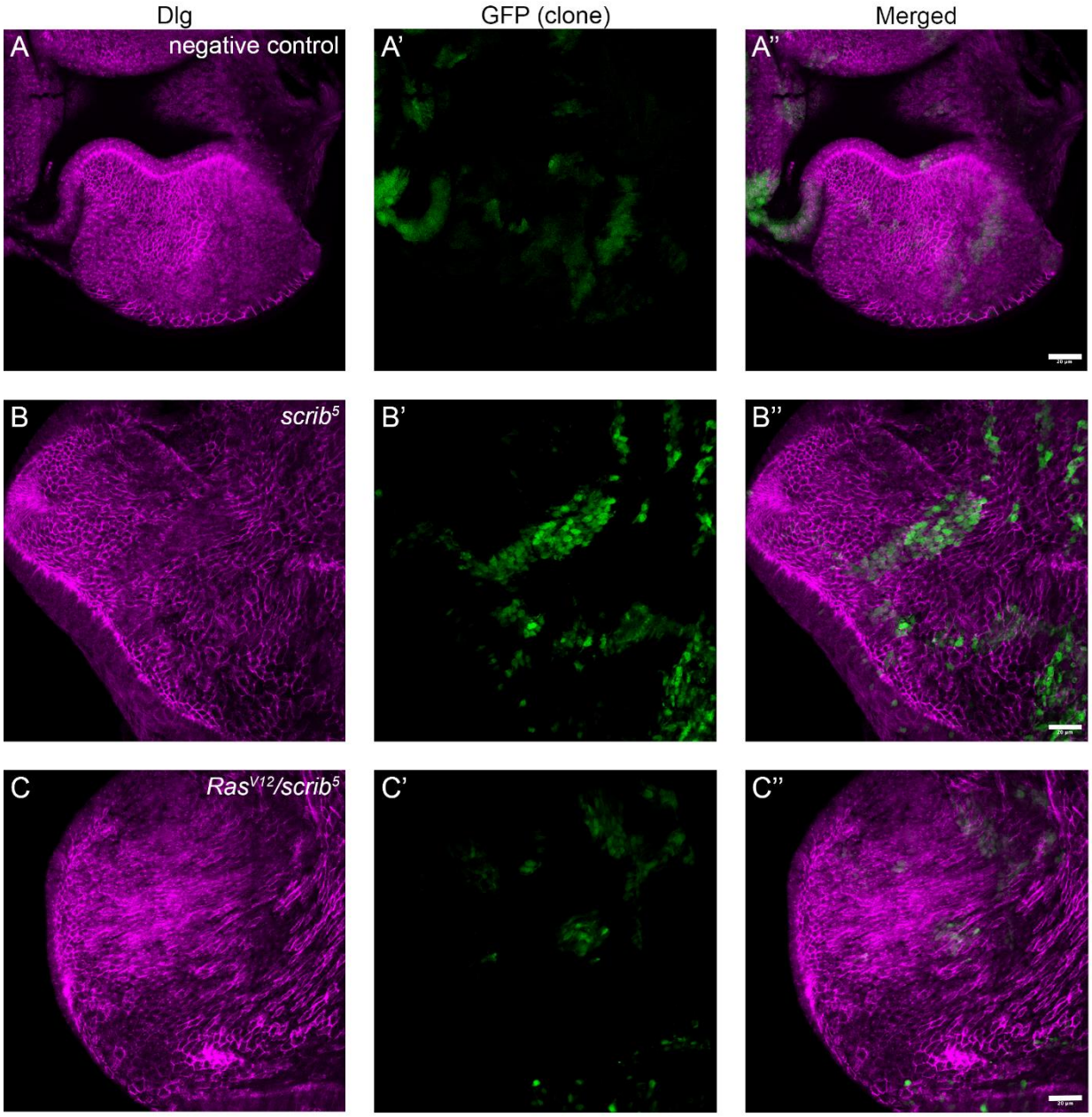

Figure 12. Image panel showing polarity in eye-antennal imaginal tissues with different genotypes. Mutant clones visualized with GFP (green) signal and Dlg (magenta) staining, indicating the apicobasal polarity of the cells via Dlg protein positioning in the cell membranes. Images were taken with the Olympus FluoView 1000 confocal microscope, using a 60x objective. (A–A'') Eye-antennal disc with control clones. (B–B'') *scrib*^{5} and (C–C'') *Ras*^{V12}*/scrib*^{5} mutant clones in the eye-antennal disc. Scale bars: 20 μm.

2.4 Discussion

Apico-basal polarity (ABP) is a key element for the structural integrity and function of epithelial tissues (Knust, 2000). Tumour suppressor genes (TSGs), including neoplastic TSGs (nTSGs) such as *scribble*, play a crucial role in maintaining ABP and controlling cell proliferation. Loss of *scrib* function has been associated with both overproliferation and loss of polarity in the *Drosophila* imaginal disc tissues (Wodarz & Näthke, 2007).

Previous studies have indicated that the $scrib^5$ allele behaves in a context-dependent manner. While $scrib^5$ clones are surrounded by wild-type cells, the mutated protein appears sufficient to maintain ABP and control cell proliferation. However, when $Scrib^5$ comprises the whole tissue, the tissues seem to lose polarity and show overpoliferation of the cells (Huang et al., 2023). Previous studies have also indicated synergies between activated proto-oncogene Ras^{V12} and *scrib* null allele ($scrib^1$), showing extreme overproliferation of the tissues and loss of ABP (Brumby & Richardson, 2003). The results from this study support the context-dependent behaviour of $Scrib^5$ and synergistic interaction with Ras^{V12}.

While *scrib* null mutant cells, e.g., $scrib^2$, display loss of ABP, ABP is maintained in $scrib^5$ mutant clones when they are surrounded by wild-type cells in the wing imaginal discs (Huang et al., 2023; Zeitler et al., 2004). Similar results were observed with *scrib5* clones in the eye-antennal imaginal discs, where overall tissue structure and patterning were preserved (Figure 11C–C''). The small clone size in $scrib^2$ (Figure 11B–B'') appears to reflect cell competition where WT cells eliminate mutant cells, consistent with findings by Huang et al. (2023).

Interestingly, flies harbouring $Ras^{V12}/scrib^2$ mutant clones developed into adults with severely altered eye morphology (Figure 10B; Appendix 1C). This is different from previous results reporting lethality at larval or pupal stages. One possible explanation of these differences is the varying genetic backgrounds. Since these mutant alleles, including null $scrib^1$ or $scrib^2$, have been maintained in various labs for many years, the accumulation of random mutations may affect viability when $Ras^{V12}/scrib^2$ mosaic clones are produced. This phenomenon could be examined further in future studies.

The results from this study showed synergy between Ras^{V12} and $Scrib^2$ as described by Brumby and Richardson (2003). This study further revealed a similar strong synergy between Ras^{V12} and $Scrib^5$ (Figure 11F–F''). Co-expression of Ras^{V12} and $Scrib^5$ led to pronounced tissue overgrowth and the absence of the morphogenetic furrow (MF), indicating a failure in differentiation. Tissue expressing Ras^{V12} and $Scrib^5$ formed multi-layered, disorganized structures, more severe than those expressing Ras^{V12} alone. Dlg mislocalization in these tissues

further confirmed the loss of ABP. These results indicate that $Scrib^{5}$ is insufficient to maintain ABP and control cell proliferation in the presence of onogenic Ras, resulting in a more aggressive tumour-like phenotype.

These results demonstrate that $Scrib^{5}$ behaves differently depending on its cellular context. While it may maintain ABP when surrounded by WT cells, it fails to do so when co-expressed with Ras^{V12}. The synergy between $Scrib^{5}$ and Ras^{V12} enhances neoplastic growth and disrupts tissue organization, supporting the hypothesis that $Scrib^{5}$ is insufficient to counteract oncogenic signalling and prevent tumour progression.

2.4.1 Future prospects

The co-expression of Ras^{V12} and $Scrib^{5}$ has not been investigated before, which formed the basis for the aims of this thesis. The results provide valuable information for future research. While $Scrib^{5}$ mutant clones alone appear capable of maintaining ABP in the eye-antennal disc tissues, the combination of Ras^{V12} and $Scrib^{5}$ results in a loss of ABP and deregulated cell proliferation. The results of this thesis indicate a synergistic interaction between Ras^{V12} and $Scrib^{5,}$ leading to overproliferation and disruption of epithelial organization. This highlights a potential connection between oncogenes and polarity protein function, which may be important for understanding tumor development and progression. Future studies would explore this interaction in more detail. Furthermore, testing this in other model organisms would help determine whether similar interactions occur in the vertebrate system.

CONCLUSIONS

The MARCM system for the generation of mutant clones has been demonstrated to be a powerful tool for investigating the roles of specific genotypes in *Drosophila melanogaster* eye-antennal imaginal discs. This system allows observation of mutant clone behaviour within the tissue and their impact on tissue morphology in a whole organism. The main goal of this thesis was to elucidate how the mutated *scrib* allele, $scrib^{5}$, and the activated proto-oncogene Ras^{V12} affect the eye-antennal imaginal disc tissues. This study specifically focused on determining whether these mutations act synergistically to promote overproliferation and disrupt apicobasal polarity, thereby forming a more pronounced tumour-like phenotype than Ras^{V12} alone, or whether $Scrib^{5}$ retains the ability to maintain ABP and regulate cell proliferation.

The results in this thesis showed that the co-expression of Ras^{V12} and $Scrib^{5}$ results in significantly enlarged, multi-layered eye-antennal imaginal disc tissues, accompanied by highly irregular future eye development. These results indicate a strong synergistic interaction between Ras^{V12} and $Scrib^{5}$, leading to more enhanced, overproliferated eye-antennal imaginal disc tissues. The widespread loss of cell polarity in tissues expressing both mutations supports the conclusion that this genetic interaction promotes neoplastic transformation and potentially metastatic behaviour.

Overall, this study highlights the insufficiency of $Scrib^{5}$ to maintain epithelial polarity in the presence of oncogenic Ras^{V12}, underscoring the importance of cooperative interactions between oncogenes and tumour suppressor genes in both development and disease. These insights contribute to a deeper understanding of the molecular mechanisms underlying tumorigenesis and provide a valuable foundation for future research into the Scribble protein and its role in epithelial tissue regulation.

***scribble* alleelide rolli uurimine Ras-indutseeritud kasvaja tekkes *Drosophila melanogaster*'i silma-tundla imaginaaldiskides**

Laura Elisabeth Christel Lään

Resümee

Apiko-basaalne polaarsus (ABP) on üks olulisemaid epiteelirakkude omadusi, tagades epiteelkudede struktuuri ja funktsioneerimise. Mitmeid loomariigis konserveerunud faktorid on rakkude ABP säilimiseks üliolulised. Näiteks tuumor suppressorgeenid, neist neoplastilised tuumor suppressorgeenid Scribble (Scrib), Disc-large ja Lethal giant larvae võivad defektsena põhjustada rakkude proliferatsiooni häireid ja ABP kadu. Kasvajarakkudel on enamasti apiko-basaalne polarisatsioon häiritud ning neile on omane kontrollimatu rakkude proliferatsioon. Uurimaks kasvajate kujunemise mehhanisme on üheks võimaluseks kasutada äädikakärbse mudelit. Äädikakärbes, *Drosophila melanogaster* on kujunenud heaks mudelorganismiks erinevatel teadusaladel nagu arengubioloogia, geneetika ja neurobioloogia, tänu tema lühikesele generatsiooniajale, kompaktsele genoomile, mis sisaldab homolooge imetajate genoomis ning üpris odavatele majanduskuludele. Tekitades uuritava geeni suhtes mutantseid kloonrakke arenevates sihtmärkkudedes, näiteks imaginaaldiskides, on võimalik uurida vastavates kudedes toimuvaid patoloogilisi muutusi. Käesolevas töös kasutati mutantsete kloonide genereerimiseks MARCM süsteemi, mille tulemusel moodustuvad FLP/FRT põhjustatud mitootilise rekombinatsiooni tulemusel rohelist fluorestseeruvat valku (GFPd) ekspresseerivad rakud ehk mutantsed kloonrakud. Käesolevas bakalaureusetöös keskenduti erinevatele Scribble mutantsetele vormidele (Scribble^{2}, Scribble^{5}) ja nende ko-ekspressioonile pidevalt aktiveeritud proto-onkogeeni Ras^{V12}-ga. Antud uurimuse peamiseks eesmärgiks oli välja selgitada, kas mutantne Scrib^{5} on võimeline säilitama silma-tundla imaginaaldiskides kudede homöostaasi ja ABPd kui seda ekspresseeritakse koos aktiveeritud onkogeeni Ras^{V12} samas kloonis või toimivad need sünergiliselt, mõjutades võimendatult kasvaja-laaadsete muutuste tekkimist arenevates silma-tundla kudedes võrrelduna olukorraga kui on ekspresseritud ainult Ras^{V12}.

Bakalaureusetöö tulemustest selgus, et silma-tundla imaginaaldiskides, milles tekitatud kloonid ekspresseerisid samaaegselt nii aktiveeritud Ras^{V12} kui ka Scrib^{5}, tekkis intensiivne koe vohamine ja rakkude ABP kadu. Areneva silma-tundla kudede struktuur ja muster oli muutunud ning silma-tundla imaginaaldiskid olid märgatavalt suuremad võrreldes metsiktüüpi ja ainult mutantseid Ras^{V12} kloone sisaldavate imaginaaldiskidega. Tulemused kinnitasid püstitatud

hüpoteesi, et Scrib^{5} ja Ras^{V12} toimivad sünergiliselt, põhjustades silma-tundla imaginaaldiski rakkude kontrollimatut proliferatsiooni, ABP kadumist ja kasvaja-laadsete struktuuride moodustumist. Lisaks leiti, et Scrib^{5} ei piisa ABP säilimiseks kui on ekspresseeritud koos onkogeeni Ras^{V12}-ga silma-tundla imaginaaldiskides.

REFERENCES

Atkins, M., & Mardon, G. (2009). Signaling in the third dimension: The peripodial epithelium in eye disc development. *Developmental Dynamics*, *238*(9), 2139–2148. https://doi.org/10.1002/dvdy.22034

Bilder, D. (2004). Epithelial polarity and proliferation control: Links from the *Drosophila* neoplastic tumor suppressors. *Genes & Development*, *18*(16), 1909–1925. https://doi.org/10.1101/gad.1211604

Bilder, D., Li, M., & Perrimon, N. (2000). Cooperative Regulation of Cell Polarity and Growth by *Drosophila* Tumor Suppressors. *Science*, *289*(5476), 113–116. https://doi.org/10.1126/science.289.5476.113

Bilder, D., & Perrimon, N. (2000). Localization of apical epithelial determinants by the basolateral PDZ protein Scribble. *Nature*, *403*(6770), 676–680. https://doi.org/10.1038/35001108

Blair, S. S. (2003). Genetic mosaic techniques for studying Drosophila development. *Development*, *130*(21), 5065–5072. https://doi.org/10.1242/dev.00774

Bonello, T. T., & Peifer, M. (2019). Scribble: A master scaffold in polarity, adhesion, synaptogenesis, and proliferation. *Journal of Cell Biology*, *218*(3), 742–756. https://doi.org/10.1083/jcb.201810103

Bosco, G., Campbell, P., Leiva-Neto, J. T., & Markow, T. A. (2007). Analysis of Drosophila Species Genome Size and Satellite DNA Content Reveals Significant Differences Among Strains as Well as Between Species. *Genetics*, *177*(3), 1277–1290. https://doi.org/10.1534/genetics.107.075069

Brand, A. H., & Perrimon, N. (1993). Targeted gene expression as a means of altering cell fates and generating dominant phenotypes. *Development*, *118*(2), 401–415. https://doi.org/10.1242/dev.118.2.401

Brumby, A. M., & Richardson, H. E. (2003). Scribble mutants cooperate with oncogenic Ras or Notch to cause neoplastic overgrowth in Drosophila. *The EMBO Journal*, *22*(21), 5769–5779. https://doi.org/10.1093/emboj/cdg548

Bryant, D. M., & Mostov, K. E. (2008). From cells to organs: Building polarized tissue. *Nature Reviews Molecular Cell Biology*, *9*(11), 887–901. https://doi.org/10.1038/nrm2523

Demerec, M., & Kaufman, B. P. (1996). *Drosophila Guide* (10. tr). Carnegie Institution of Washington. https://archive.org/details/ciw-drosophila-guide-10/page/n1/mode/2up

Dorot, O., Steller, H., Segal, D., & Horowitz, M. (2017). Past1 Modulates Drosophila Eye Development. *PLOS ONE*, *12*(1), e0169639. https://doi.org/10.1371/journal.pone.0169639

Ernst, A., Appleton, B. A., Ivarsson, Y., Zhang, Y., Gfeller, D., Wiesmann, C., & Sidhu, S. S. (2014). A Structural Portrait of the PDZ Domain Family. *Journal of Molecular Biology*, *426*(21), 3509–3519. https://doi.org/10.1016/j.jmb.2014.08.012

Flores-Benitez, D., & Knust, E. (2016). Dynamics of epithelial cell polarity in Drosophila: How to regulate the regulators? *Current Opinion in Cell Biology*, *42*, 13–21. https://doi.org/10.1016/j.ceb.2016.03.018

Fortini, M. E., Simon, M. A., & Rubin, G. M. (1992). Signalling by the sevenless protein tyrosine kinase is mimicked by Rasl activation. *Nature*, *355*(6360), 559–561. https://doi.org/10.1038/355559a0

Germani, F., Bergantinos, C., & Johnston, L. A. (2018). Mosaic Analysis in Drosophila. *Genetics*, *208*(2), 473–490. https://doi.org/10.1534/genetics.117.300256

Gimple, R. C., & Wang, X. (2019). RAS: Striking at the Core of the Oncogenic Circuitry. *Frontiers in Oncology*, *9*, 965. https://doi.org/10.3389/fonc.2019.00965

Hales, K. G., Korey, C. A., Larracuente, A. M., & Roberts, D. M. (2015). Genetics on the Fly: A Primer on the *Drosophila* Model System. *Genetics*, *201*(3), 815–842. https://doi.org/10.1534/genetics.115.183392

Halfar, K., Rommel, C., Stocker, H., & Hafen, E. (2001). Ras controls growth, survival and differentiation in the *Drosophila* eye by different thresholds of MAP kinase activity. *Development*, *128*(9), 1687–1696. https://doi.org/10.1242/dev.128.9.1687

Huang, Y., Gui, J., Myllymäki, S.-M., Mikkola, M. L., & Shimmi, O. (2023). Coordination of tissue homeostasis and growth by the Scribble-α-Catenin-Septate junction complex. *iScience*, *26*(4), 106490. https://doi.org/10.1016/j.isci.2023.106490

Karim, F. D., Chang, H. C., Therrien, M., Wassarman, D. A., Laverty, T., & Rubin, G. M. (1996). A Screen for Genes That Function Downstream of Ras1 During Drosophila Eye Development. *Genetics*, *143*(1), 315–329. https://doi.org/10.1093/genetics/143.1.315

Karim, F. D., & Rubin, G. M. (1998). Ectopic expression of activated Ras1 induces hyperplastic growth and increased cell death in Drosophila imaginal tissues. *Development*, *125*(1), 1–9. https://doi.org/10.1242/dev.125.1.1

Knust, E. (2000). Control of epithelial cell shape and polarity. *Current Opinion in Genetics & Development*, *10*(5), 471–475. https://doi.org/10.1016/S0959-437X(00)00115-5

Lee, T., & Luo, L. (2001). Mosaic analysis with a repressible cell marker (MARCM) for Drosophilaneural development. *Trends in Neurosciences*, *24*(5), 251–254. https://doi.org/10.1016/S0166-2236(00)01791-4

Matsumoto, K., Toh-e, A., & Oshima, Y. (1978). Genetic control of galactokinase synthesis in Saccharomyces cerevisiae: Evidence for constitutive expression of the positive regulatory gene gal4. *Journal of Bacteriology*, *134*(2), 446–457. https://doi.org/10.1128/jb.134.2.446-457.1978

Miles, W. O., Dyson, N. J., & Walker, J. A. (2011). Modeling tumor invasion and metastasis in *Drosophila*. *Disease Models & Mechanisms*, *4*(6), 753–761. https://doi.org/10.1242/dmm.006908

Millburn, G. H., Crosby, M. A., Gramates, L. S., Tweedie, S., & the FlyBase Consortium. (2016). FlyBase portals to human disease research using *Drosophila* models. *Disease Models & Mechanisms*, *9*(3), 245–252. https://doi.org/10.1242/dmm.023317

Miller, D. E., Cook, K. R., Arvanitakis, A. V., & Hawley, R. S. (2016). Third Chromosome Balancer Inversions Disrupt Protein-Coding Genes and Influence Distal Recombination Events in *Drosophila melanogaster*. *G3 Genes|Genomes|Genetics*, *6*(7), 1959–1967. https://doi.org/10.1534/g3.116.029330

Miller, D. E., Cook, K. R., & Hawley, R. S. (2019). The joy of balancers. *PLOS Genetics*, *15*(11), e1008421. https://doi.org/10.1371/journal.pgen.1008421

Miller, D. E., Cook, K. R., Hemenway, E. A., Fang, V., Miller, A. L., Hales, K. G., & Hawley, R. S. (2018). The Molecular and Genetic Characterization of Second Chromosome Balancers in *Drosophila melanogaster*. *G3 Genes|Genomes|Genetics*, *8*(4), 1161–1171. https://doi.org/10.1534/g3.118.200021

Mirzoyan, Z., Sollazzo, M., Allocca, M., Valenza, A. M., Grifoni, D., & Bellosta, P. (2019). Drosophila melanogaster: A Model Organism to Study Cancer. *Frontiers in Genetics*, *10*, 51. https://doi.org/10.3389/fgene.2019.00051

Osterfield, M., Berg, C. A., & Shvartsman, S. Y. (2017). Epithelial Patterning, Morphogenesis, and Evolution: Drosophila Eggshell as a Model. *Developmental Cell*, *41*(4), 337–348. https://doi.org/10.1016/j.devcel.2017.02.018

Parvathi V, D., Amritha, A., & Solomon, F. D. P. (2009). Wonder animal model for genetic studies—Drosophila melanogaster—Its lifecycle & Breeding methods – A review. *Sri Ramachandra Journal of medicine*, *2*(2), 33–38.

Prober, D. A., & Edgar, B. A. (2000). Ras1 Promotes Cellular Growth in the Drosophila Wing. *Cell*, *100*(4), 435–446. https://doi.org/10.1016/S0092-8674(00)80679-0

Roote, J., & Prokop, A. (2017). How to design a genetic mating scheme: A basic training package for Drosophila genetics. *figshare. Journal contribution*. https://doi.org/10.6084/m9.figshare.106631.v34

Salzberg, A., Cohen, N., Halachmi, N., Kimchie, Z., & Lev, Z. (1993). The *Drosophila Ras2* and *Rop* gene pair: A dual homology with a yeast *Ras* -like gene and a suppressor of its loss-of-function phenotype. *Development*, *117*(4), 1309–1319. https://doi.org/10.1242/dev.117.4.1309

St Johnston, D., & Sanson, B. (2011). Epithelial polarity and morphogenesis. *Current Opinion in Cell Biology*, *23*(5), 540–546. https://doi.org/10.1016/j.ceb.2011.07.005

Stebbins, M. J., & Yin, J. C. P. (2001). Adaptable doxycycline-regulated gene expression systems for Drosophila. *Gene*, *270*(1–2), 103–111. https://doi.org/10.1016/s0378-1119(01)00447-4

Zeitler, J., Hsu, C. P., Dionne, H., & Bilder, D. (2004). Domains controlling cell polarity and proliferation in the *Drosophila* tumor suppressor Scribble. *The Journal of Cell Biology*, *167*(6), 1137–1146. https://doi.org/10.1083/jcb.200407158

Zhang, Q., Wang, Y., Bu, Z., Zhang, Y., Zhang, Q., Li, L., Yan, L., Wang, Y., & Zhao, S. (2024). Ras promotes germline stem cell division in Drosophila ovaries. *Stem Cell Reports*, *19*(8), 1205–1216. https://doi.org/10.1016/j.stemcr.2024.06.005

Tepass, U., Tanentzapf, G., Ward, R., & Fehon, R. (2001). Epithelial Cell Polarity and Cell Junctions in *Drosophila*. *Annual Review of Genetics*, *35*(1), 747–784. https://doi.org/10.1146/annurev.genet.35.102401.091415

Ugur, B., Chen, K., & Bellen, H. J. (2016). *Drosophila* tools and assays for the study of human diseases. *Disease Models & Mechanisms*, *9*(3), 235–244. https://doi.org/10.1242/dmm.023762

Vidal, M., & Cagan, R. L. (2006). Drosophila models for cancer research. *Current Opinion in Genetics & Development*, *16*(1), 10–16. https://doi.org/10.1016/j.gde.2005.12.004

Wang, C., Jamal, L., & Janes, K. A. (2012). Normal morphogenesis of epithelial tissues and progression of epithelial tumors. *WIREs Systems Biology and Medicine*, *4*(1), 51–78. https://doi.org/10.1002/wsbm.159

Weasner, B. P., & Kumar, J. P. (2022). The early history of the eye-antennal disc of *Drosophila melanogaster*. *Genetics*, *221*(1), iyac041. https://doi.org/10.1093/genetics/iyac041

Wodarz, A., & Näthke, I. (2007). Cell polarity in development and cancer. *Nature Cell Biology*, *9*(9), 1016–1024. https://doi.org/10.1038/ncb433

Younossi-Hartenstein, A., Tepass, U., & Hartenstein, V. (1993). Embryonic origin of the imaginal discs of the head of Drosophila melanogaster. *Roux's Archives of Developmental Biology*, *203*(1–2), 60–73. https://doi.org/10.1007/bf00539891

USED WEBSITES

Abcam. (1998-2025). Accessed on 13.05.2025 https://www.abcam.com/en-us

Bloomington Drosophila Stock Center. (2021). From Indiana University Bloomington. Accessed on 08.05.2025 https://bdsc.indiana.edu/index.html

DSHB. (1986 – 2025). Accessed on 13.05.2025 https://dshb.biology.uiowa.edu/

Proteintech Group. (2002-2025). Accessed on 10.05.2025 https://www.ptglab.com/news/blog/the-importance-of-blocking-when-using-nano-secondary-reagents-for-if/#:~:text=Blocking%20is%20an%20essential%20step,even%20mask%20the%20specific%20signal

APPENDICES

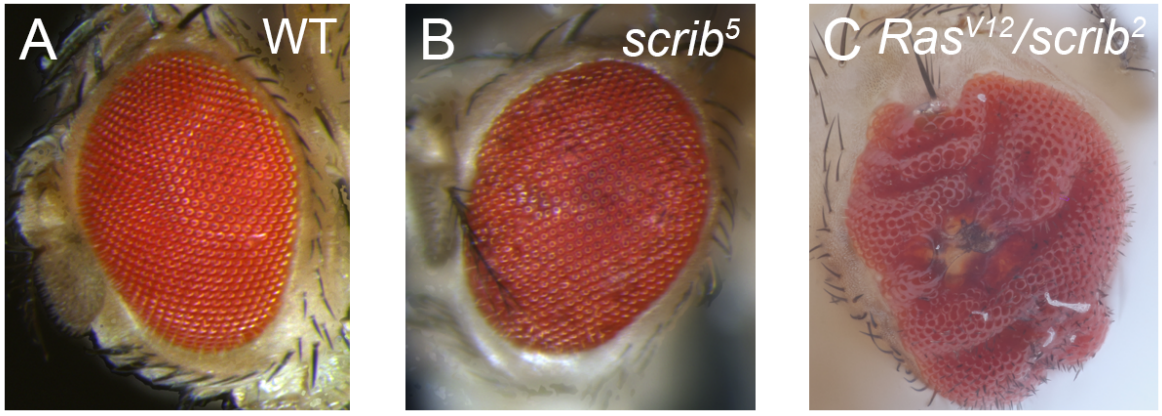

Appendix 1. Additional images of the adult eye phenotypes. (A) Wild-type (WT) fly's eye, showing regular structure and patterning. (B) Milder phenotype of an eye (minor alterations in the patterning of ommatidia), with *scrib*^{5} mutant clones. (C) Severely affected eye (mutant clones with *Ras*^{V12} and *scrib*^{2} together) exhibiting a strongly folded neoplastic phenotype. Images were acquired using the Leica M165 fluorescent stereo microscope equipped with a Leica DFC450 C camera. (Images A and B obtained by lab associate Tamara Rudman)

Non-exclusive license for reproducing the thesis and making the thesis available to the public

I, Laura Elisabeth Christel Lään,

1. grant the University of Tartu a free permit (non-exclusive license) to reproduce, for the purpose of preservation, including for adding the thesis to the DSpace digital archives until the expiry of the term of copyright, my thesis

   "Investigating the role of *scribble* alleles in Ras-induced tumorigenesis in *Drosophila melanogaster* eye-antennal imaginal discs"

   supervised by Professor Osamu Shimmi and Associate Professor Tambet Tõnissoo;

2. I grant the University of Tartu permission to make the thesis specified in point 1 available to the public via the online environment of the University of Tartu, including via the DSpace digital archives, under the Creative Commons license CC BY NC ND 4.0, which allows, by giving appropriate credit to the author, to reproduce, distribute the work and communicate it to the public, and prohibits the creation of derivative works and any commercial use of the work until the expiry of the term of copyright;

3. I am aware that the rights specified in points 1 and 2 also remain for the author;

4. I confirm that by granting the non-exclusive license, I do not violate other individuals' intellectual property rights or the rights arising from the personal data protection legislation.

Laura Elisabeth Christel Lään

26.05.2025